Formation and Geochemical Significance of Iron Bog Deposits

By Mark R. Stanton, Douglas B. Yager, David L. Fey, and Winfield G. Wright

Chapter E14 of
Integrated Investigations of Environmental Effects of Historical Mining in the Animas River Watershed, San Juan County, Colorado
Edited by Stanley E. Church, Paul von Guerard, and Susan E. Finger

Professional Paper 1651

U.S. Department of the Interior
U.S. Geological Survey

Contents

Abstract 693
Introduction and Background 693
Field and Analytical Methods 694
Study Area, Geology and Alteration Types, and Sample Localities 694
Solid Phase Chemistry 696
Sample Collection, Preparation, and Analysis 696
Mineralogy 696
Element Abundances 697
Carbon Abundance, Isotopic Dating (^{14}C), and Composition 697
Aqueous Chemistry 697
Sample Collection, Preparation, and Analysis 697
Reconnaissance Study 697
Detailed Study of the Upper Bog of Cement Creek 698
Biological Characterization 698
Iron and Sulfur Oxidizing Bacteria 698
Photosynthetic Organisms 699
Geochemical Modeling 699
Results 699
Solid Phase Chemistry of Iron Oxyhydroxide 699
Location and Size of Iron Deposits 699
Mineralogy 700
Major and Trace Elements in Solids 700
Core Samples 700
Bonner Waste Pile 700
Carbon Abundance, Ages, and Composition 701
Aqueous Chemistry 702
Water Composition—All Sites 702
Surface Water Versus Ground Water—All Sites 702
Surface Water Versus Ground Water—Upper Bog of Cement Creek 706
Ratio of Fe^{2+} to Fe_{tot} 706
Dissolved Oxygen as an Indicator of Ground Water 707
Trace-Element Chemistry and Alteration Type 708
Microbial Populations 708
Geochemical Modeling 710
Discussion 711
Geochemical Evolution of Meteoric and Surface Water to Iron Bog Ground Water 711
Geochemical Evolution of Iron Bog Ground Water to Iron Bog Surface Water 711
Iron Oxidation 713
Formation of Iron Oxyhydroxide and Schwertmannite 713
Mineralogy of Iron Bog Solids 714
Location of Precipitation of Solid Phases 714
Solid Phase Chemistry Versus Alteration Type 715
Trace-Element Composition of Iron Oxyhydroxide 715
Water Chemistry Versus Alteration Type 715

Accumulation of Iron Oxyhydroxide 716
Formation of Modern "Waste-Pile Ferricrete" Deposits 716
Role of Photosynthetic Organisms 717
Estimated Rates of Iron Oxyhydroxide Deposition 718
Carbon Preservation within Iron Bogs 718
References Cited 718

Figures

1. Map of Animas River watershed study area, showing generalized rock units and geologic contacts, areas of dominant alteration types, major drainages, sample site localities, and types of samples collected at each locality 695
2. Photograph showing outlet at south end of lower bog in Cement Creek basin 697
3. Downhole plot of major- and trace-element abundances, Core 97ABS327 from the red spring of Prospect Gulch 701
4. Downhole plot of major- and trace-element abundances, Core 999291 from South Fork Mineral Creek 703
5–7. Box plots of major- and trace-element concentrations, and water chemistry parameters in the following:
    5. Surface and ground water, all iron depositional sites 705
    6. Surface and ground water, upper bog of Cement Creek 706
    7. Zero DO (ground) water, upper bog of Cement Creek, and nonzero DO (surface) water from all other sites 708
8. Photograph of *Leptothrix* film on water surface at lower bog of Cement Creek 711
9. Graph showing postulated evolution of ground water to surface water using data from upper bog of Cement Creek 712
10. Graph showing relationship of aqueous concentrations of iron and aluminum in all iron depositional environments 716
11. Photograph showing moss layer and relict algal filaments retaining iron oxyhydroxide near Cascade Gulch adit, Cement Creek 717

Tables

1. Examples of X-ray diffraction results from iron bog or spring samples, Animas River watershed study area, showing types of iron-bearing, nonsilicate minerals 700
2. Summary statistics for major- and trace-element abundances in core and mine-waste iron oxyhydroxide samples 702
3. Sample site and location, deposit and alteration type, water type, major- and trace-element concentration, water chemistry parameter, Fe^{2+}/Fe_{tot} ratio, and range (minimum, maximum) of detectable concentrations for all water samples 704
4. Median values of major-element concentrations, trace-element concentrations, and water chemistry parameters according to separation of water types where iron is actively being deposited 704
5. Summary statistics of major- and trace-element concentrations, and water chemistry parameters in surface and ground water, all iron depositional sites 705
6. Summary statistics of major- and trace-element concentrations, and water chemistry parameters in surface and ground water (based on positive hydraulic head), and nonzero DO and zero DO water, upper bog Cement Creek 707
7. Results of Most Probable Number (MPN) culturing for *Thiobacillus* species in iron bogs, Animas River watershed study area 710

Chapter E14
Formation and Geochemical Significance of Iron Bog Deposits

By Mark R. Stanton, Douglas B. Yager, David L. Fey, and Winfield G. Wright

Abstract

Aqueous and solid phase geochemistry of actively forming iron bogs in the Animas River watershed study area near Silverton, Colorado, suggests that all iron bogs (whether active or inactive) in the study area formed in a similar manner. Geochemical modeling of analytical data demonstrates that oxidation of ferrous iron (transported in low-pH, low dissolved oxygen ground water) to ferric iron is the mechanism common to the formation of these iron deposits. The change in oxidation state causes precipitation of fine-grained iron oxyhydroxide solids near the point of ground-water discharge. Local geology, parent rock mineralogy, alteration type, ground-water composition, geochemically active microbes and plants, and depositional-site geochemistry are among the major factors that influence the formation, growth, and persistence of the iron bogs.

According to this genetic model, ground water circulating through the regional rock mass acquires dissolved ferrous iron via dissolution of abundant sulfide minerals (primarily pyrite) in the country rock. This acid weathering produces high concentrations of aqueous species such as aluminum and calcium from host silicate minerals, and copper and zinc from metal-rich sulfide minerals. Maximum concentrations of aqueous iron, aluminum, and sulfate are 140, 22.1, and 910 milligrams per liter, respectively. Maximum concentrations of the trace elements copper, lead, zinc, and arsenic are Cu 18,000, Pb 110, Zn 53,000, and As 4,300 micrograms per liter.

Upon emergence at the surface, ferrous iron is oxidized to ferric iron by dissolved atmospheric or biogenic molecular oxygen [O_2(aq)], or iron-oxidizing microbes. Ferric iron then reacts to form fine-grained, texturally homogeneous crystalline phases and noncrystalline (amorphous) chemical precipitates. In iron bogs, the amorphous material generally constitutes more than 50 weight percent of the solids.

The crystalline iron oxyhydroxides are mainly goethite (α-FeOOH) and schwertmannite ($Fe_8O_8(OH)_6SO_4$). The mixed crystalline-amorphous solids are iron rich with varying concentrations of aluminum, sulfate, and trace elements. Iron and aluminum reach concentrations as high as 46.0 and 12.1 weight percent, respectively. Trace-element contents are dependent on the parent rock mineralogy and alteration type drained by ground water. Maximum concentrations of copper, lead, zinc, and arsenic in different iron bog solids are Cu 110, Pb 60, Zn 660, and As 5,000 parts per million. Thus, iron bogs have the capacity to act as reservoirs and perhaps sources of several major and trace elements.

The largest volumetric accumulations of iron oxyhydroxide are produced by iron bog and iron spring deposits; seeps and mine adit/waste-pile drainages form smaller accumulations. Iron mobilization and deposition in iron bogs in the Animas River watershed has been occurring for about the last 9,000 years, a fact supported by carbon-14 (^{14}C) dating on relict carbon from the iron bogs.

Introduction and Background

Fine-grained, mostly clast free iron oxyhydroxide deposits are present in several areas of the Animas River watershed study area in southwestern Colorado. These deposits have been mapped by D.B. Yager and others (Yager and Bove, this volume, Chapter E1, pl. 2); most are classified as iron bogs because of their low-pH water and their location in water-saturated, relatively level terrain such as stream valley bottoms (Gore, 1983). Other iron-depositing environments, such as springs and seeps, and mine adit or waste-pile drainages, also are found throughout the area. These sites of iron deposition are usually located where ground water may have reached the surface, as, along structures or fractures, or where ground water intersects surface flows (streams).

An understanding of the origin, composition, and evolution of the variety of iron-rich deposits has several applications. First, because iron bogs are potential sinks or sources of large concentrations of many major and trace metals (Church and others, 1997), it is important to examine how these deposits form and persist (or degrade) in the Animas River watershed. Second, knowledge of how the deposits form can yield

useful information concerning geochemical processes related to acid-rock and acid-mine drainage generation, and the potential effect these processes have on water quality. Finally, geochemical processes operating in modern-day iron bogs may be analogous to those that form the iron oxide cement of clast-bearing ferricrete found in the area (Wirt and others, this volume, Chapter E17; Verplanck and others, this volume, Chapter E15).

One process fundamental to an understanding of iron bog formation and geochemistry is precipitation of the solid phase. The oxidation of Fe^{2+} to Fe^{3+} by dissolved atmospheric oxygen is slow under acidic conditions, having half-times as long as 2–3 years (Stumm and Morgan, 1985; Singer and Stumm, 1970). The concentration of dissolved iron in iron bog water (as much as 70 mg/L) is such that chemical oxidation by dissolved O_2(aq) alone will not convert all Fe^{2+} to Fe^{3+} rapidly (a few days). Thus, a suitable oxidant in addition to O_2(aq) is probably involved in forming iron oxyhydroxide deposits in low-pH water (Carlson and Kumpulainen, 2000). Bacteria have been implicated in a number of studies as important oxidants of ferrous iron (Bigham and others, 1990).

Bacteria of the genus *Thiobacillus* are potential agents for accelerating the rate of iron and sulfur oxidation in low-pH environments (Nordstrom and Southam, 1997; Bigham, 1994). The two prominent species are *Th. ferrooxidans*, a ferrous iron-oxidizing bacterium, and *Th. thiooxidans*, a reduced-sulfur oxidizing bacterium. *Leptothrix* is another bacterium that is an indicator of iron oxidation, but whether it truly oxidizes Fe^{2+} under acidic conditions has not yet been established (van Veen and others, 1978).

A variety of iron minerals can be formed via oxidation of ferrous iron under acidic conditions present in the iron bogs. Schwertmannite (iron oxyhydroxysulfate; $Fe_8O_8(OH)_6SO_4$) typically forms over the pH range 3 to 4. Goethite (iron oxyhydroxide; α-FeOOH) is known to form over a wider pH range (3.5 to 8.0). At sulfate concentrations less than 1,000 mg/L and pH less than 6.0, goethite can form directly from solution (Carlson and Kumpulainen, 2000). Goethite also forms via recrystallization and drying of initially hygroscopic, amorphous and crystalline iron oxyhydroxides such as ferrihydrite ($Fe(OH)_3$). For simplicity, the crystalline (goethite, schwertmannite, ferrihydrite) and amorphous iron-aluminum-sulfate-rich solids in iron bogs will be collectively referred to as iron oxyhydroxide in this chapter. Hematite (iron oxide, Fe_2O_3) may form by dehydration and recrystallization of precursor iron phases such as goethite or ferrihydrite; it is the thermodynamically stable iron oxide in iron bog environments. However, several kinetic and physicochemical factors control whether hematite, goethite, or other iron-bearing solids will form and remain stable in the iron bogs.

Iron bogs are considered active when water is present on the surface, issues from the base or sides of the deposit, or in some cases, collects in moderate-sized pools. (Most of the active bogs can be considered "iron fens"; however, because other depositional sites had been subject to surface water contributions, inactive ("dry") for more than a year, or influenced by anthropogenic activities, a more encompassing term of "iron bog" was employed to describe these sites.) An inactive iron bog is one with a dry surface and no water issuing from the base or sides. Plants on an inactive bog may be dormant, dead, or completely absent depending on the length of time the bog has been inactive. The designation of an iron bog as active or inactive carries no precise age significance, only that water was present or absent from the site when visited. At some sites, an active iron bog is adjacent to an inactive one as a result of migration of water that reaches the site. Because aqueous data were not obtainable from inactive bogs, this chapter focuses on the characteristics of active, modern iron bog environments.

The geochemical, mineralogical, microbiological, and depositional characteristics are used to develop genetic models that can be compared to help identify formation mechanisms. Our model indicates that the iron oxyhydroxide component in all types of iron-bearing deposits forms via the same fundamental mechanism. However, some aspects of this model remain uncertain, such as the origin and evolution of the ferrous iron-bearing ground water, magnitude and types (regional versus local) of ground-water flow paths, and specific rates of ground-water flow and iron deposition. The results illustrate that iron oxyhydroxide deposition has been occurring in the region for several thousands of years. The end result of the depositional process is the formation of iron bogs that can act as short- and long-term reservoirs (or sources) of major and trace elements in the Animas River watershed study area.

Field and Analytical Methods

Study Area, Geology and Alteration Types, and Sample Localities

The Animas River watershed study area (fig. 1) covers approximately 500 km^2 (25 km E.-W. by 20 km N.-S.); the area is subdivided into three drainage basins: Mineral Creek, Cement Creek, and upper Animas River. The study area of this chapter (dotted rectangle, fig. 1) includes Cement Creek from 5 km below its headwaters in Ross Basin to its confluence with the Animas River, South Fork Mineral Creek west and outside of the Silverton caldera margin, and Mineral Creek from its confluence with South Fork Mineral Creek to its headwaters near Red Mountain Pass. Figure 1 shows the sites where samples described in this chapter were collected.

Figure 1 (facing page). Animas River watershed study area, showing generalized rock units and geologic contacts, areas of dominant alteration types, major drainages, sample site localities, and types of samples collected at each locality. Dotted rectangle, area of study of this chapter. Drainage map modified from Church and others (1997).

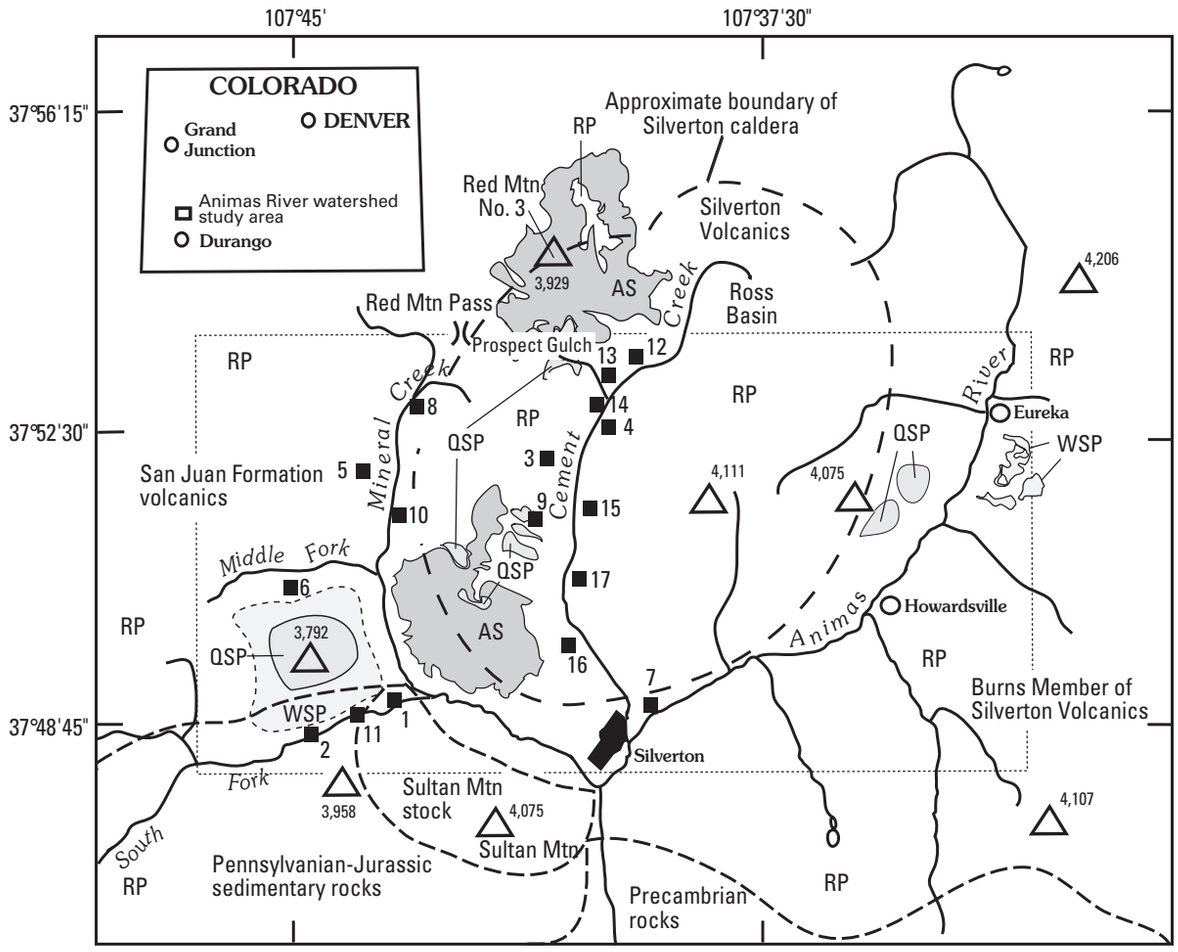

Site No.	Drainage	Site name and (or) description	Samples collected
1	SFMC	Iron bog	*S, *GW, SW
2	SFMC	Wetland (organic)	S, GW, SW, M
3	CC	Seep	S, SW
4	CC	Upper iron bog	*S, *GW, *SW, *M
5	MC	Imogene adit drainage	S, SW, M
6	MC	Bonner mine waste pile drainage	S, *GW, *SW, M
7	AR	Mine-waste pile (dry)	S
8	MC	Junction mine adit, iron bog	*S, GW, *SW, *M
9	CC	Topeka Gulch spring deposit	S, SW, M
10	MC	Seep, iron bog	S, GW, *SW
11	SFMC	Iron bog	*S(c), *GW, *SW, *M
12	CC	Seep N. of Prospect Gulch	SW
13	CC	Red spring iron bog, Prospect Gulch	*S(c), *GW, *SW, *M
14	CC	Seep SE. of Prospect Gulch	SW
15	CC	Cascade Gulch adit	---
16	CC	Lower iron bog	---
17	CC	Yukon tunnel	---

SFMC, South Fork Mineral Creek; MC, Mineral Creek; CC, Cement Creek; AR, Animas River.
S, sediment; S(c), sediment core; GW, ground water; SW, surface water; M, microbiological.
(*), multiple samples of this type taken at site; (---), no samples collected at site.

Hydrothermal alteration associated with mineral deposits in the area produced suites of minerals that represent gradational differences in intensity of alteration (Bove and others, this volume, Chapter E3). Regional propylitization (RP) is the weakest grade, and minerals are primarily altered feldspars with little or no sulfides except pyrite. Weak sericite-pyrite (WSP) is low-grade alteration where the pyrite has low metal contents. Quartz-sericite-pyrite (QSP) is medium- to high-grade alteration; these minerals have metal abundances generally higher than do WSP alteration minerals (but variable). The highest grade alteration is acid-sulfate (AS), characterized by abundant metal-rich sulfide minerals. Vein-related quartz-sericite-pyrite altered minerals (V-QSP alteration; Bove and others, this volume) are present on an areally restricted, smaller scale compared to the other four alteration assemblages; therefore, V-QSP alteration is not considered separately here. Tetrahedrite, galena, sphalerite, and chalcopyrite are the primary ore minerals in the deposits in the region (Bove and others, this volume). A highly generalized depiction of rock types, areas of dominant alteration types, and geologic contacts is in figure 1.

South Fork Mineral Creek drains several alteration types: WSP/QSP-altered rocks of the subeconomic porphyry copper-molybdenum deposit on and near peak 3,792 m (hosted by lower Oligocene San Juan Formation volcanics) to the north, unaltered Pennsylvanian-Permian redbeds through Jurassic sedimentary rocks south and west of peak 3,792 m, and altered and unaltered San Juan Formation volcanics farther west (Yager and Bove, this volume, pl. 1). Across South Fork Mineral Creek (southeast of peak 3,792 m) is the porphyritic Sultan Mountain stock (Oligocene age), an intrusive approximating quartz monzonite-diorite composition (Yager and Bove, this volume).

The Mineral Creek basin also drains multiple alteration types, from unaltered RP and WSP/QSP type rocks along its western border to dominantly AS and QSP altered rocks to the east and north.

Cement Creek is dominated on the west and north by acid-sulfate and QSP-altered rocks of the Silverton Volcanics (Oligocene) that make up the Silverton caldera, whose margins are approximated by the large circular outline in figure 1. Rocks east of Cement Creek are mainly propylitically altered with scattered zones of WSP and QSP alteration.

Along the upper Animas River are rocks of the Burns Member of the Silverton Volcanics, which are dominantly propylitically altered with small areas of WSP east of the river and QSP west of the river. The Silverton Volcanics are host rocks for most of the mineral deposits in the Animas River watershed study area north and east of the South Fork of Mineral Creek area (Lipman and others, 1973). See Yager and Bove (this volume, pl. 1), and Bove and others (this volume) for a detailed summary of the geology and alteration types in the area.

Solid Phase Chemistry

Sample Collection, Preparation, and Analysis

Sediment (iron oxyhydroxide; core or surface), ground water, surface water, and microbiological samples were collected at each site (when possible) in the study area (fig. 1). The active iron-deposition sites include iron bogs (fig. 2), springs, seeps, and mine drainages (adits or waste piles). Organic-rich wetlands can be sites of limited iron deposition but are compositionally different from iron deposits; they are described in Stanton, Fey, and others (this volume, Chapter E25).

Surficial unindurated iron oxyhydroxide samples (<1–5 cm thick) were removed with a spatula; indurated surface samples were dislodged using a cold chisel and small sledgehammer. Subsurface samples most commonly were taken as cores by driving a 0.5 to 1.5 m length of 5-cm diameter PVC pipe into the sediment. Cores were measured for recovery and then closed off from the air by sealing the ends with PVC caps. In instances where coring was unworkable (highly indurated sediment), a shallow trench (<1 m) was dug to obtain subsurface material. Grab samples were stored in polyethylene bags until processed in the lab approximately 2 weeks after collection.

Subsamples from cores were taken at 1 cm intervals to provide adequate analytical coverage. If present, large clasts were hand-separated; all sediment was sieved to less than 63 mesh to remove sand-sized grains and macroscopic organic matter. Iron oxyhydroxide was generally fine grained and homogeneous, but detrital grains smaller than 63 mesh were not removed by sieving. Sediment was air-dried if damp, split, then powdered to <230 mesh (57 µm (micrometers)) using a ceramic mortar and pestle or shatterbox for use in subsequent analyses.

Mineralogy

X-ray diffractometry (XRD) was used to examine mineralogy of iron oxyhydroxide. A packed powder mount prepared from the <230 mesh sample was scanned using Ni-filtered Cu K_{α} radiation. The detection limit of a mineral with this method is approximately 5 weight percent.

The crystalline phase designations of major, minor, and trace, and estimations of amorphous material, were obtained by using the background intensity of the diffractograms relative to the intensities of the crystalline phases in the unknown sample (for amorphous material), and to the intensities of pure phases relative to their intensities in the unknown sample (for crystalline material). The designations (in weight percent) of major (>25), minor (≥5 to ≤25), and trace (<5) abundances are derived from the difference of 100 percent crystalline material minus the estimated amorphous material. Major, minor, and trace designations indicate only qualitative amounts and relative abundances of crystalline or amorphous solids detected.

Figure 2. Outlet at south end of lower bog in Cement Creek basin. Surface dimensions of this iron bog are approximately 60 m long by 6 m wide. In common with other active iron bogs, this deposit is characterized by abundant fine-grained iron oxyhydroxide, living organisms (for example, the mosses near the base and on the surface), relict organic matter, and a lack of large clasts. Visible part of steel spatula is approximately 10 cm long.

Element Abundances

A split of the <230 mesh sample was analyzed by inductively coupled plasma–atomic emission spectrometry (ICP-AES) for 40 major and trace elements. Sample preparation involves sequential digestion using hydrochloric, nitric, perchloric, and hydrofluoric acids. Details of the analytical technique, apparatus, and detection limits can be found in Briggs (2002).

Carbon Abundance, Isotopic Dating (^{14}C), and Composition

To see whether ^{14}C dating could be applied to determine the age of the deposits, aliquots of the <230-mesh solid samples were analyzed for total carbon ($C_{(tot)}$), organic carbon ($C_{(org)}$), and carbonate (mineral) carbon ($C_{(min)}$) by induction furnace methods (Brown and Curry, 2002; Curry, 1990). Most iron oxyhydroxide samples did contain sufficient organic carbon to employ ^{14}C dating and carbon isotopic composition ($\delta^{13}C$) methods that were later performed at a commercial laboratory. The uppermost layers (approximately 0.5 m) of iron bogs with visible, recently deposited organic matter were not dated, as they would show only modern dates. The ages are important to constrain the time of formation of the iron bogs, but an extensive discussion of the role of carbon in the geochemical evolution of the iron bogs is not within the scope of this chapter. Tabulation of the ^{14}C dating results are in Verplanck and others, this volume; Vincent and Elliott, this volume, Chapter E22; and Vincent and others, this volume, Chapter E16.

Aqueous Chemistry

Sample Collection, Preparation, and Analysis

Reconnaissance Study

Reconnaissance water sampling at multiple sites was undertaken to determine the aqueous geochemistry of different environments where iron deposition was actively occurring. To adequately compare and contrast the different environments, 26 water samples from 11 localities were collected and analyzed. Sample sites include four iron bogs, three adit or waste-pile drainages, seven seeps (three associated with the upper bog of Cement Creek), and two spring deposits (fig. 1).

One organic bog (wetland; site 2) was included in the sampling (but not in the statistical calculations) to allow comparison of the iron-rich deposits to a low-iron system. Three other sites were visited and described but no samples were collected (sites 15, 16, and 17).

Samples were collected from water flowing across the surface, issuing from the base or sides of larger deposits, from pools in larger bogs, or where fresh iron oxyhydroxide was visible (for example, seeps along Cement Creek). At some localities, water was collected using a "sniffer," a simple well-point device equipped with Teflon tubing that can extract ground water and indicate if hydraulic head is present (Wanty, 2000). After the device was driven through the solids into the iron bog subsurface (about 1 m maximum depth), the area penetrated was allowed to stabilize for approximately 5 minutes (as evidenced by clearing of the water); the well was developed by drawing five volumes (20 mL each) of water through the sample collection loop and discarding, and then the ground or surface water sample was collected. Where head measurements could not be made, designation of water type was based on whether the discharging water contained detectable dissolved oxygen (surface water) or no detectable dissolved oxygen (ground water). Lack of measurable dissolved oxygen was later found to be characteristic of ground water.

Samples were drawn into a 60-mL (milliliter) low-density polyethylene syringe, then filtered through a 0.45 µm polycarbonate filter into a hydrochloric acid (HCl)-washed, deionized-water-rinsed, high-density polyethylene bottle. For cations, the filtered samples were acidified to pH <2 with concentrated nitric acid (HNO_3); for anions, no further treatment after filtration was necessary. Alkalinities were not measured, as all but three samples had pH <5.0, and so no carbonate species should be present. The cation aliquots were analyzed for 44 elements by inductively coupled plasma–mass spectrometry (ICP-MS; Lamothe and others, 2002).

Total iron (Fe_{tot}) and ferrous iron (Fe^{2+}) were determined on-site within 15 minutes of filtration using a portable spectrophotometer operating at 510 nm (nanometer) wavelength (Theodorakos, 2002); ferric iron (Fe^{3+}) was determined by difference ($Fe^{3+} = Fe_{tot} - Fe^{2+}$). These values were used to calculate the ratio of ferrous to total iron (Fe^{2+}/Fe_{tot}). Aqueous sulfate (SO_4^{2-}) was determined at eight sites using the Hach method (Hach Chemical Company, 1996) and on all samples 2 weeks later by ICP-MS. The field and laboratory sulfate analyses agreed to within ±10 percent (data not shown).

Dissolved oxygen (DO, ppm), pH (standard units), temperature (°C), and specific conductance or conductivity (SpC; microsiemens/centimeter, µS/cm) were measured using meters calibrated with standards 5–10 minutes before field sampling. Measurements of pH on filtered and unfiltered aliquots to check the possible effect of colloidal iron showed no significant differences between the two sample types. The pH values agreed within ±5 percent for both measurements (data not shown).

Detailed Study of the Upper Bog of Cement Creek

To examine short-term (≤24 hours) changes in aqueous geochemistry, the upper bog along Cement Creek was studied in detail (site 4, fig. 1). The upper bog is an areally extensive (approximately 30 m long by 6 m wide) iron bog on the west bank of Cement Creek southeast of Prospect Gulch. During a day-long operation and in a subsequent sampling, numerous samples were collected along the long dimension (parallel to stream flow) where ground water would be most likely discharging into the bog. Based on the presence of a positive hydraulic head in the sniffer device, samples from the upper bog were separated into ground (head present) or surface (no head present) water. However, because the head was often small (2.5–7 cm), it could not be considered an infallible indicator of ground or surface water.

Sample collection, preparation, and analysis were the same as in the reconnaissance study. All samples were collected in July and August, the active time of snowmelt, rainfall, and runoff processes. During these months, biogeochemical processes and shallow and deep ground-water flow that could influence iron mobility are most likely to be occurring.

Biological Characterization

Iron and Sulfur Oxidizing Bacteria

Isolation and enumeration by Most Probable Number (MPN) culturing techniques (Gerhardt and others, 1994) was undertaken at eight sites to determine populations of *Thiobacillus* species. A 1.0 g (gram) raw sample of wet iron oxyhydroxide sediment was placed into a tube with 9 mL of aqueous medium and disaggregated by shaking for 5 minutes. This inoculation was defined as the first in a series of dilution tubes (10^0). One milliliter from this tube was used to inoculate other dilution tubes (from 10^{-1} to 10^{-5}) containing the aqueous medium specifically formulated to enhance the growth of the microbes (Atlas, 1995). For *Th. ferrooxidans*, a reduced iron source ($FeSO_4$) was used; for *Th. thiooxidans*, a reduced sulfur source (thiosulfate, $S_2O_3^{2-}$) was used. Tubes were inoculated on-site, then incubated at 37°C upon return to the lab. After 2 weeks, 1 month, and 2 months growth, the tubes were scored for the presence (increased turbidity) or absence (no increase in turbidity) of growth. Stained slide preparations were made from tubes that showed positive signs of growth to confirm the presence of bacteria and examine their morphology.

Geochemical reactions attributed to iron-related bacteria (IRB) were determined at selected sites using standard test kits (Biological Activity Reagent Tests or BART's; Hach Chemical Co., 1997). The tests do not distinguish among different genera of iron oxidizers but can be used as confirmatory evidence of their presence. One bacterial genus that would be among those determined by these tests is *Leptothrix*. At each site, the presence or absence of *Leptothrix* was noted, but no

attempts were made to isolate or enumerate this microbe by culture techniques. The medium was inoculated with a 1 mL unfiltered aqueous sample from the iron bog, incubated at room temperature (25°C), and checked daily over a 2-week period for either a (+) result (reddening of the originally clear medium) or a (–) result (no color change). Both sets of results (MPN and BART) are qualitative measures of the numbers of bacteria present at a site.

Photosynthetic Organisms

Associated with most iron-depositing environments are photosynthetic macro and micro organisms which grow on the surface, in pooled water, and adjacent to the boundaries of the deposit. These are mosses, cyanobacteria, algae, and small vascular plants (Yager and Bove, this volume, pl. 2, figs. 7 and 14). Observations of these different organisms at several sites were made to look for systematic similarities or differences in the flora. The organisms might act as physical or geochemical agents by stabilizing the growing iron oxyhydroxide layers, acting as traps or sorbents for iron oxyhydroxide, or providing dissolved oxygen (molecular O_2) as an oxidant of aqueous ferrous iron. In addition, the relict forms of carbon, particularly organic carbon, measured in these bogs probably originated from these organisms. Therefore, the different organisms are potentially significant to the growth and geochemical evolution of the iron bogs.

Riparian zone plants also were cataloged at eight sites during the study of the iron deposits. These include conifers, deciduous trees, woody shrubs, grasses, and sedges. The riparian zone plant data are not presented here but can be found in the database chapter (Sole and others, this volume, Chapter G).

Geochemical Modeling

Inverse geochemical modeling was employed to help us understand processes responsible for the formation of the iron bogs. Inverse modeling attempts to assess chemical evolution of ground and surface water, and any associated solid phases, along a flow path. The water compositions and parameters (pH, specific conductance (SpC), temperature) of the active upper bog of Cement Creek were first used with NETPATH (Plummer and others, 1992) to examine the possible distributions of major elements within solid phases that could form along a flow path beginning in ground water and ending in surface water. The NETPATH results were then used as data for PHREEQEC (Parkhurst and Plummer, 1995; Allison and others, 1991) to examine precipitation processes that may be taking place in the iron bog water. (Thermodynamic data for the schwertmannite modeling were provided by D.L. Parkhurst and Laurie Wirt, written commun., 2002.)

Modeling results were used to help constrain the type of water that favors formation of the minerals observed by X-ray diffraction. Model comparison with actual data was based primarily on mineralogical compositions determined by X-ray diffraction. That is, if a mineral predicted by the model results was detected by X-ray diffraction, this was considered supportive evidence that the model was fundamentally correct for that mineral.

Results

Solid Phase Chemistry of Iron Oxyhydroxide

Location and Size of Iron Deposits

Some iron deposits form where springs or seeps discharge on slopes or at breaks in slope and cause local cementation of material. These deposits form by continued accumulation of iron oxyhydroxide with little added clastic content, except the material immediately underneath the layer(s) of iron oxyhydroxide. Often, this growth results in the formation of long, wide iron oxyhydroxide "ribbons" in gullies or "curtains" adhering to steep slopes or even cliff faces. In this chapter, these iron oxyhydroxide ribbons and curtains are considered spring deposits.

Spring and seep deposits appear to form in a similar manner; the primary difference between these two environments is that seeps have lower discharge volumes and produce much smaller accumulations of iron solids than bogs or springs. Iron oxyhydroxide also accumulates where mine adit or waste-pile discharges reach the surface. Based on the absence of reworked and (or) transported clasts, spring, seep, and adit/pile discharge deposits have been classified as subtypes of iron bog deposits (Verplanck and others, this volume).

The surficial and volumetric accumulations of the different iron deposits have a wide range. For example, seeps produce small thin accumulations of iron oxyhydroxide at the surface (<1 m^2; 0.1 to <1 cm thick); mine adit/pile drainage deposits generally contain moderate accumulations (1–100 m^2; 0.5 cm–1.0 m thick); most iron bogs provide major accumulations (≤180 m^2; ≤2 m thick; fig. 2). Spring deposits display the widest range in accumulations: some cover surfaces of a few hectares and have thicknesses estimated at 3–5 m. Site 10 on Mineral Creek (fig. 1) was one of these large spring deposits, yet it had only a few small volumes of water discharging to the surface when sampled.

A distinctive type of deposit, referred to as "waste pile ferricrete," forms when mined waste rock becomes cemented by iron oxyhydroxide. Such deposits are important indicators of modern, rapid formation of iron oxyhydroxide cement and are discussed later in this chapter.

Mineralogy

Table 1 shows example results for iron minerals and their relative abundances from different iron bog or spring samples. (These samples were collected at a variety of locations in the area and do not necessarily coincide with the sites shown in fig. 1.) Most samples were mixtures of crystalline and amorphous material, but in some cases, the solids were either all crystalline or all amorphous material. For example, in several fresh surface samples, no crystalline iron-bearing phases were detected (sample SV-FFC; table 1). Crystalline mineral phases identified by X-ray analysis generally make up 0–25 weight percent of the solids; the remaining amorphous material that cannot be identified by X-ray diffraction is iron and sulfate rich (Desborough and others, 1999). Additional X-ray diffraction results are in the database (Sole and others, this volume).

Goethite and schwertmannite were the dominant iron-bearing minerals in both active and inactive iron bogs. The two minerals were generally present as minor (≥5 to ≤25 wt. percent) components of the total solids; in many samples, one mineral was relatively more abundant than the other. Of six iron bog samples, goethite was the dominant iron-bearing mineral in three (and the only crystalline phase in two of these samples), whereas schwertmannite was dominant in the other three (table 1).

Schwertmannite was the primary crystalline component of iron precipitates on streambed and iron bog surfaces, and was present in varying abundance at depth in iron bogs (≤3 cm). Hematite was not present in any sample.

Quartz was the major rock-forming (silicate) mineral. Other silicates included kaolinite, orthoclase, and muscovite, and secondary (weathered) clinochlore and montmorillonite.

Table 1. Examples of X-ray diffraction results from iron bog or spring samples, Animas River watershed study area, showing types of iron-bearing, nonsilicate minerals.

[Rock-forming minerals such as quartz were present in most samples. Iron minerals or solids are listed in approximate order from highest to lowest relative abundance]

Sample No.	Sample type	Iron minerals
IDY0014	Iron bog	Schwertmannite, goethite.
IDY00-29A	Iron bog	Schwertmannite, goethite, jarosite.
SDY0017A	Iron bog	Goethite.
95-ABS-119	Iron bog	Goethite.
99ABFC-141B	Iron bog	Schwertmannite, goethite.
99VMS-65A	Iron spring, inactive	Goethite, schwertmannite.
97-ABS-318C	Iron bog, 3 cm depth	Schwertmannite, goethite.
99ABFC-154C	Iron spring, active	Amorphous iron oxyhydroxide.
SV-FFC	"Filamentous" iron oxide attached to algal mass.	Amorphous iron oxyhydroxide.

Major and Trace Elements in Solids

The median and range (minima, maxima) are the principal measures used for comparison of major- and trace-element concentrations and physiochemical parameters in sediment and water. Geochemical data generally do not exhibit normal distributions (Till, 1974), and in our data, lognormal or bimodal distributions were seen. In such distributions, samples with very high (Junction mine; site 8, fig. 1, AMLI mine site # 77) or very low (Topeka Gulch; site 9, fig. 1) concentrations would exaggerate mean values.

Core Samples

Data from Core 97ABS327, from the red spring at the lower end of Prospect Gulch (site 13, fig. 1), show iron and aluminum concentrations typical of active iron bogs. In individual samples from this core, iron ranges from 6.4 to 46.0 wt. percent and aluminum ranges from 0.4 to 6.1 wt. percent (fig. 3; table 2), with median values of 36.0 wt. percent iron and 1.8 wt. percent aluminum over the entire core.

Trace-element ranges (table 2) show copper above the detection limit of 1 ppm in only 14 of 69 samples. However, in the interval of 20–30 cm, eight contiguous samples had relatively high copper. Lead was detectable in 61 of 68 samples, and zinc and arsenic were detected in every sample. Of particular interest is the high median arsenic content of 2,700 ppm.

Core 999291 was taken on South Fork Mineral Creek about 1.3 km before it meets main Mineral Creek (site 11, fig. 1). Iron and aluminum ranges were 2.9–41.0 and 2.2–7.5 wt. percent, respectively (fig. 4). Respective median values for iron and aluminum over the entire core were 27.0 and 4.2 wt. percent.

Trace elements in core 999291 show a marked contrast to the samples in core 97ABS327 from Prospect Gulch. Copper was detectable in all but 5 samples and zinc was detected in all samples, but lead was detected in only 11 samples and arsenic in only 8 samples. These two cores demonstrate that although iron and aluminum concentrations tend to be similar in iron bog solids, trace-element enrichment can differ widely.

Bonner Waste Pile

The sample of iron oxyhydroxide cement from the Bonner mine waste pile (AMLI mine site # 172; table 2) shows iron present at the same maximum abundance (46.0 wt. percent) as in the red spring core. However, aluminum is markedly lower (0.05 wt. percent) in the Bonner sample than in either of the two cores. Copper, lead, zinc, and arsenic were all at detectable levels, which again points out the variability of iron oxyhydroxide enrichment with respect to deposit-related elements.

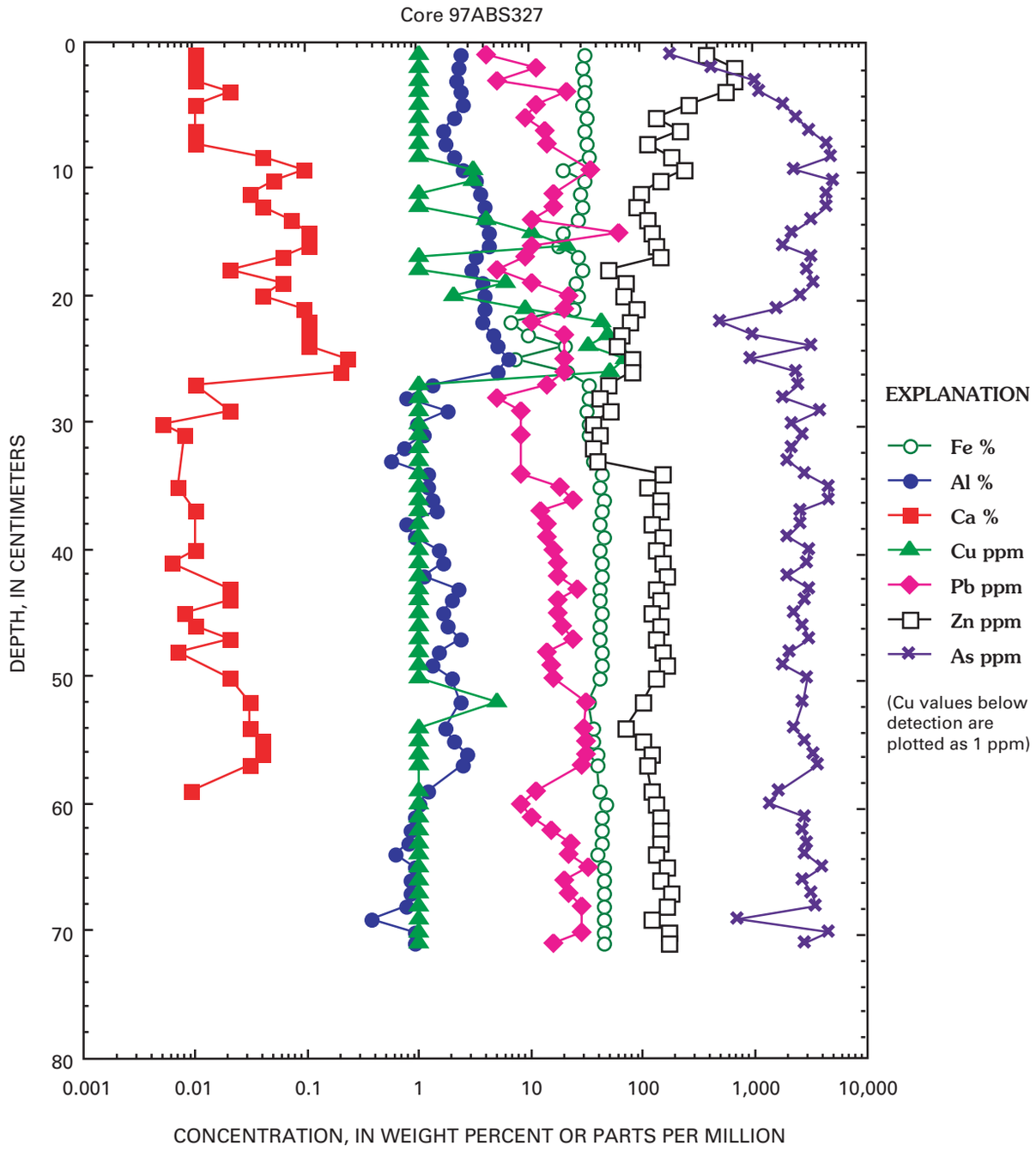

Figure 3. Downhole plot of major- (Al, Fe, Ca (wt. percent)) and trace- (Cu, Pb, Zn, As (ppm)) element abundances, Core 97ABS327 from red spring of Prospect Gulch.

Carbon Abundance, Ages, and Composition

Iron oxyhydroxide samples taken from below about 0.5 m contained low concentrations of all forms of carbon; in these deeper samples, total carbon (the sum of organic plus mineral carbon) usually did not exceed 1 wt. percent. However, organic carbon in samples above 0.5 m from active iron bogs routinely exceeded 30 wt. percent.

The ^{14}C ages of all iron deposits (including ferricretes) range from approximately 9,200 years before present (yr B.P.) to 1,200 yr B.P. (Verplanck and others, this volume; Vincent and others, this volume). However, we do not know whether organic matter in iron oxyhydroxide represents all "old" carbon originally deposited in the bog, or a mixture of modern and old carbon deposited as the bog formed. The ^{14}C dates do signify that old carbon has been deposited and (or) preserved

Table 2. Summary statistics for major- (Al, Fe, Ca (wt. percent)) and trace- (Cu, Pb, Zn, As (ppm)) element abundances in core and mine-waste iron oxyhydroxide samples.

[ND*, not determined because 70 percent or more of samples were below detection. <LLD, below lower limit of detection]

	Al	Fe	Ca	Cu	Pb	Zn	As
Core 97ABS327, red spring of Prospect Gulch							
n	68	68	46	14	61	68	68
Minimum	0.4	6.4	0.005	<LLD	4.0	35	180
Maximum	6.1	46.0	0.2	70	61	660	5,000
Median	1.8	36.0	0.02	ND*	16	130	2,700
Core 999291, South Fork Mineral Creek							
n	35	35	35	30	11	35	8
Minimum	2.2	2.9	0.02	1.0	<LLD	25	<LLD
Maximum	7.5	41.0	3.0	110	24	430	29
Median	4.2	27.0	0.1	9.5	ND*	40	ND*
Bonner mine-waste pile, Middle Fork Mineral Creek							
One sample	0.05	46.0	<LLD	61	15	46	54

in the iron deposits, rather than having been completely oxidized and removed. The presence of relict wood and algal structures preserved in many iron oxyhydroxide samples suggests that old organic carbon was preserved in the matrix of the iron precipitates.

Carbon isotopic analyses that show most $\delta^{13}C$ values fall within the expected range for terrestrial plants ($-27^0/_{00}$ (per mil) to $-34^0/_{00}$) such as those found in the iron bogs. However, several values range from $-22^0/_{00}$ to $-26^0/_{00}$, suggesting an algal component ($-12^0/_{00}$ to $-23^0/_{00}$; Hoefs, 1980). The amount, if any, of fresh (modern) organic carbon that has been added to the preserved woody and algal materials is not known.

Aqueous Chemistry

An examination of differences in water compositions is a useful tool in differentiation and description of iron depositional environments. We follow this sequence of description:

1. All samples collected in this study

2. Ground water and surface water from all sites where iron is being deposited

3. Ground water and surface water from iron bogs only (excludes seeps and springs, and adit/pile drainages)

4. Ground water and surface water only from the upper bog of Cement Creek, a site of large-scale iron deposition and accumulation.

Comparisons discussed in this section are between ground water and surface water and within each type, and they include (1) concentrations of major elements, primarily Al, Fe, and S (as SO_4) but also Ca, Si, and Mn; (2) concentrations of four environmentally important trace elements (Cu, Pb, Zn, As); and (3) water chemistry parameters (pH, SpC, DO). Table 3 summarizes several characteristics of the aqueous samples.

Water Composition—All Sites

Median aqueous concentrations of water sampled from all active iron depositional sites show elevated total iron (Fe_{tot}; 40 mg/L), aluminum (15 mg/L), and sulfate (410 mg/L), and acid pH (4.2; table 4). Dissolved oxygen ranged from 0 to 7 ppm, and median specific conductance was moderately high at 870 µS/cm. Exceptions to the high dissolved iron, aluminum, and sulfate concentrations were samples from the Topeka Gulch site (site 9, fig. 1), which also had high dissolved oxygen (5.2 ppm), the Mineral Creek spring deposit (site 10, fig. 1), and the Imogene adit (site 5, fig. 1, AMLI mine site # 136). In contrast to these dilute water samples, the Junction mine sample (site 8, fig. 1) had very high aqueous concentrations of iron and the four trace elements. Ground and surface water issuing from or feeding the active iron depositional sites contained differing concentrations of other major elements such as calcium, silica, and manganese, and trace elements such as copper, lead, zinc, and arsenic (table 3).

Table 4 summarizes median concentrations of major species (iron, aluminum, sulfate) and trace elements in seven water types separated as all water from all iron depositional sites, surface water from all sites, ground water from all sites, surface water from all iron bogs, ground water from all iron bogs, surface water from the upper bog of Cement Creek, and ground water from the upper bog of Cement Creek. As table 4 shows, ground and surface water compositions from all iron bogs are very similar to those of the upper bog of Cement Creek. Therefore, the discussion of iron bog water chemistry will focus on samples from the upper bog.

Surface Water Versus Ground Water—All Sites

The box plot in figure 5 allows for comparison of major- or trace-element concentrations in ground or surface water. Outliers (samples above the 90th percentile or below the 10th percentile) are shown as open circles. The lower

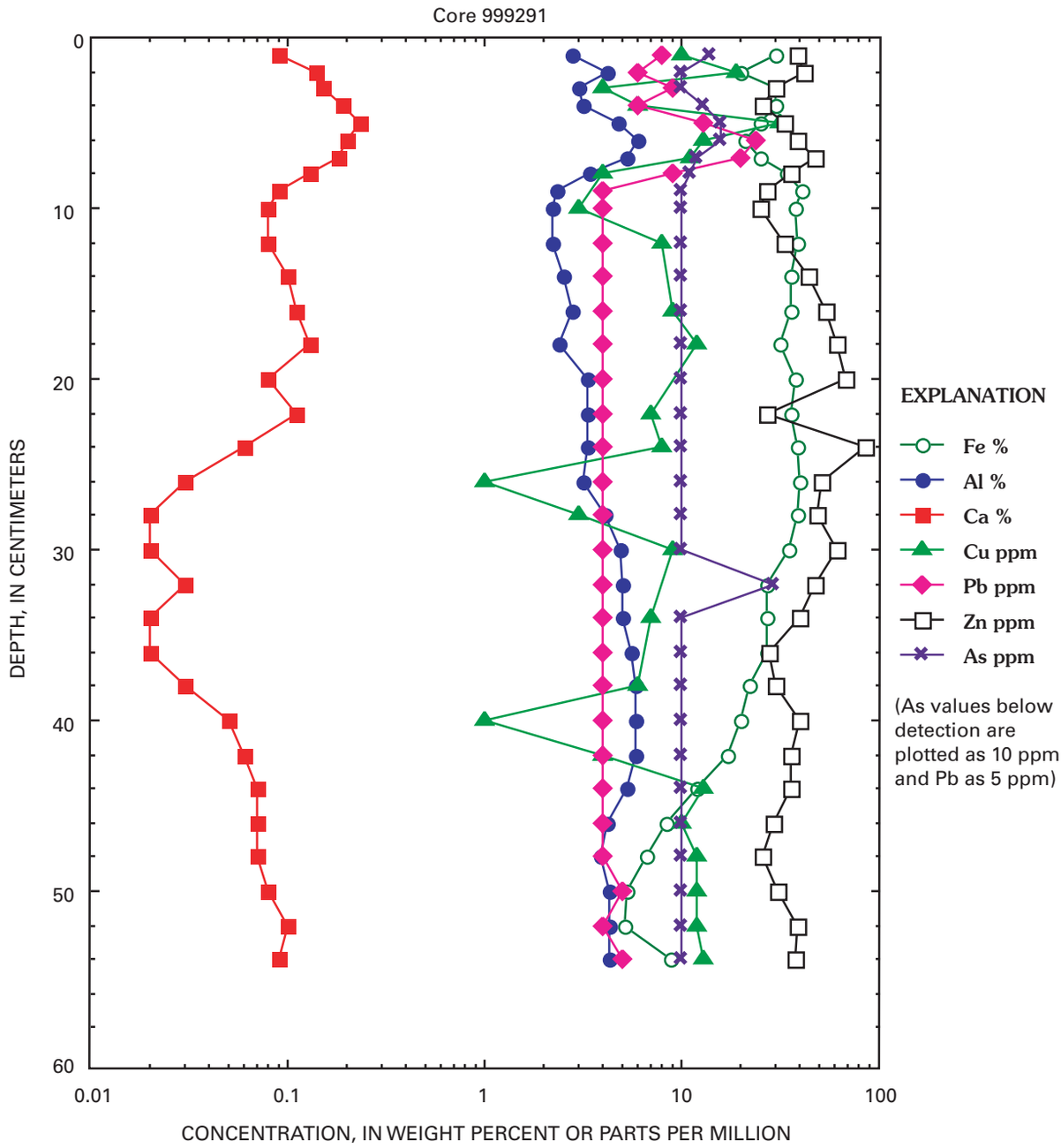

Figure 4. Downhole plot of major- (Al, Fe, Ca (wt. percent)) and trace- (Cu, Pb, Zn, As (ppm)) element abundances, Core 999291 from South Fork Mineral Creek.

and upper lines of the rectangular box represent the 25th and 75th percentiles; the horizontal line through the box is the median (50th percentile). For any particular variable, a greater vertical extent of the entire box plot indicates greater variation, whereas a short compact box plot indicates less variation.

The concentrations of dissolved species are more distinct when ground water and surface water are considered separately. Median aluminum, iron, and sulfate in ground water are nearly twice the concentrations of surface water (fig. 5; table 4). Specific conductance of ground water is higher than that of surface water, consistent with the higher concentrations of elements indicative of weathering of sulfide and silicate minerals observed in ground water (fig. 5; table 5). Median dissolved oxygen is lower in ground water than in surface water.

The Junction mine site is responsible for the high trace-element concentration outliers in figure 5. Water draining the adit at this site was considered ground water because it was derived from within the barricaded mine through a 30 m length of PVC pipe. Because dissolved oxygen could not be measured at the pipe outlet, the measurement was made on water at the iron bog 10 m downstream of the pipe.

Table 3. Sample site and location, deposit and alteration type, water type, major- (mg/L) and trace-element concentration (µg/L), water chemistry parameter, Fe^{2+}/Fe_{tot} ratio, detection limit, and range (minimum, maximum) of detectable concentrations for all water samples.

[SpC, specific conductance, in microsiemens per centimeter; DO, dissolved oxygen; NA, not analyzed or not applicable; LLD, lower limit of detection; <, less than; hydraulic head: P, positive; N, not observed; ND, not determined]

Site No.	Sample site or location	Deposit type	Alteration type[1]	Water type[2]	Fe mg/L	Al mg/L	SO_4 mg/L	Ca mg/L	Cu µg/L	Pb µg/L	Zn µg/L	As µg/L	pH units	SpC µS/cm	DO ppm	Fe^{2+}/Fe_{tot}	Hydraulic head
4	Upper bog	Fe bog	AS	g	71.9	15.9	910	270	14.5	18.5	1,740	77.1	4.30	1,510	0.0	1.00	P
4	Upper bog	Fe bog	AS	g	72.3	16.6	810	280	14.9	10.4	1,720	67.6	4.27	1,520	0.0	1.00	P
4	Upper bog	Fe bog	AS	s	69.8	17.4	900	238	9.4	3.9	1,620	49.2	4.00	1,380	3.3	.93	N
4	Upper bog	Fe bog	AS	s	69.2	17.5	820	242	13.7	33.0	1,630	44.4	4.17	1,380	ND	.99	N
4	Upper bog	Fe bog	AS	g	67.2	18.6	710	205	12.3	6.3	1,680	10.7	4.15	1,280	0.0	.99	P
4	Upper bog	Fe bog	AS	s	50.6	18.3	720	204	28.4	23.8	1,710	4.2	3.46	1,360	0.0	.94	N
4	Upper bog	Fe bog	AS	s	50.2	17.8	780	235	14.4	75.4	1,760	13.1	3.40	1,430	5.0	.62	N
4	Upper bog	Fe bog	AS	g	73.2	20.0	820	238	8.0	9.2	1,690	4.6	4.11	1,260	0.0	.98	P
4	Upper bog	Fe bog	AS	s	52.4	20.0	750	226	82.4	100.	1,710	3.0	3.41	1,410	7.0	.89	N
4	Upper bog	Fe bog	AS	g	71.6	22.1	580	134	13.6	75.5	1,620	76.3	4.47	900	0.0	.99	P
4	Upper bog	Fe bog	AS	s	31.8	6.4	390	102	26.3	28.0	590	3.0	3.19	850	7.0	.76	N
10	Mineral Creek	Spring	WSP	s	7.4	5.0	80	12.7	2.1	.83	190	2.0	4.26	210	3.5	.99	ND
3	Cement Creek	Seep	AS	g	34.5	8.7	250	49	10.6	16.2	660	3.0	4.30	440	0.0	1.00	P
3	Cement Creek	Seep	AS	s	30.4	8.3	340	51.1	11.6	29.7	630	<LLD	3.92	520	3.9	.95	N
3	Cement Creek	Seep	AS	s	2.3	1.1	380	148	18.3	2.9	650	<LLD	5.94	770	6.2	.95	ND
12	Cement Creek	Seep	AS	g	38.1	8.8	350	93.1	20.3	16.4	650	10.3	4.27	670	0.0	.99	P
12	Cement Creek	Seep	AS	g	37.6	8.7	350	91.0	8.8	37.5	640	11.2	4.26	700	0.0	.98	ND
14	Cement Creek	Seep	AS	g	35.9	9.4	270	53.0	10.1	34.9	630	11.9	4.27	520	0.0	.97	P
14	Cement Creek	Seep	AS	s	35.8	8.7	260	52.1	14.2	27.5	650	11.4	4.19	550	ND	.99	ND
1	So. Fk. Mineral	Fe bog	RP	s	30.0	16.0	230	23.0	40.0	.70	240	7.0	4.74	320	ND	ND	ND
9	Topeka Gulch	Spring	AS	s	0.2	1.8	110	39.0	7.0	<LLD	60	5.0	3.35	240	5.2	ND	ND
13	Red spring	Fe bog	AS	g	45.0	20.0	300	32.0	<LLD	.50	1,100	38.0	3.47	680	5.1	ND	ND
4	Upper bog	Fe bog	AS	g	42.0	15.0	710	200	6.0	4.0	1,500	7.0	3.37	1,310	5.8	ND	N
5	Imogene adit	Adit	RP	s	9.1	1.3	220	70.0	10.0	<LLD	420	7.0	5.87	460	ND	ND	ND
6	Bonner mine	Adit/pile	QSP	s	10.0	6.1	430	120.0	100.0	11.0	2,300	8.0	3.17	990	5.1	ND	ND
8	Junction mine	Adit/Fe bog	AS	g	140.0	19.0	870	76.0	18,000	110	53,000	4,300	2.68	1,900	*5.3	ND	ND
2	**Organic bog	Wetland	RP	s	0.5	0.9	100	39.1	8.0	<LLD	50	5.0	3.25	890	6.5	ND	ND
				LLD	<0.03	<0.1	<0.3	<0.05	<0.05	<0.05	<0.2	<2	NA	NA	0.1	NA	
				n	26	26	26	26	25	25	26	24	26	26	21	NA	
				Min	0.2	1.1	80	13	2.1	0.5	60	2.0	2.7	210	0	NA	
				Max	140.0	22.1	910	280	18,000	110	53,000	4,300	5.9	1,900	7.0	NA	

[1]RP, regional propylitic; WSP, weak sericite-pyrite; QSP, quartz-sericite-pyrite; AS, acid-sulfate.

[2]g, ground water; s, surface water; *n*, number of samples.

*Measurement taken in iron bog downstream from adit/pipe.

**Sample not used in calculation of statistical parameters.

Table 4. Median values of major-element concentrations (Al, Fe, S (as SO_4); mg/L), trace-element concentrations (Cu, Pb, Zn, As; µg/L), and water chemistry parameters according to separation of water types where iron is actively being deposited.

[SpC, specific conductance (µS/cm; microsiemens per centimeter); DO, dissolved oxygen (ppm; parts per million)]

Water type	*n*	Al	Fe	SO_4	Cu	Pb	Zn	As	pH	SpC	DO
All water	26	15.4	40.0	410	14	17	1,300	11	4.2	870	3.3
All surface water	15	8.5	31.1	390	14	26	650	7	4.0	810	5.0
All ground water	11	16.2	56.1	650	12	16	1,560	12	4.3	1,080	0
All iron bog surface water	7	17.6	50.4	730	26	26	1,620	10	3.5	1,370	5.0
All iron bog ground water	8	18.6	71.6	710	13	9	1,680	2	4.2	1,280	1.8
Upper bog surface water	6	17.6	51.5	760	20	30	1,670	9	3.4	1,380	5.0
Upper bog ground water	6	17.6	71.8	760	13	10	1,680	39	4.2	1,290	0

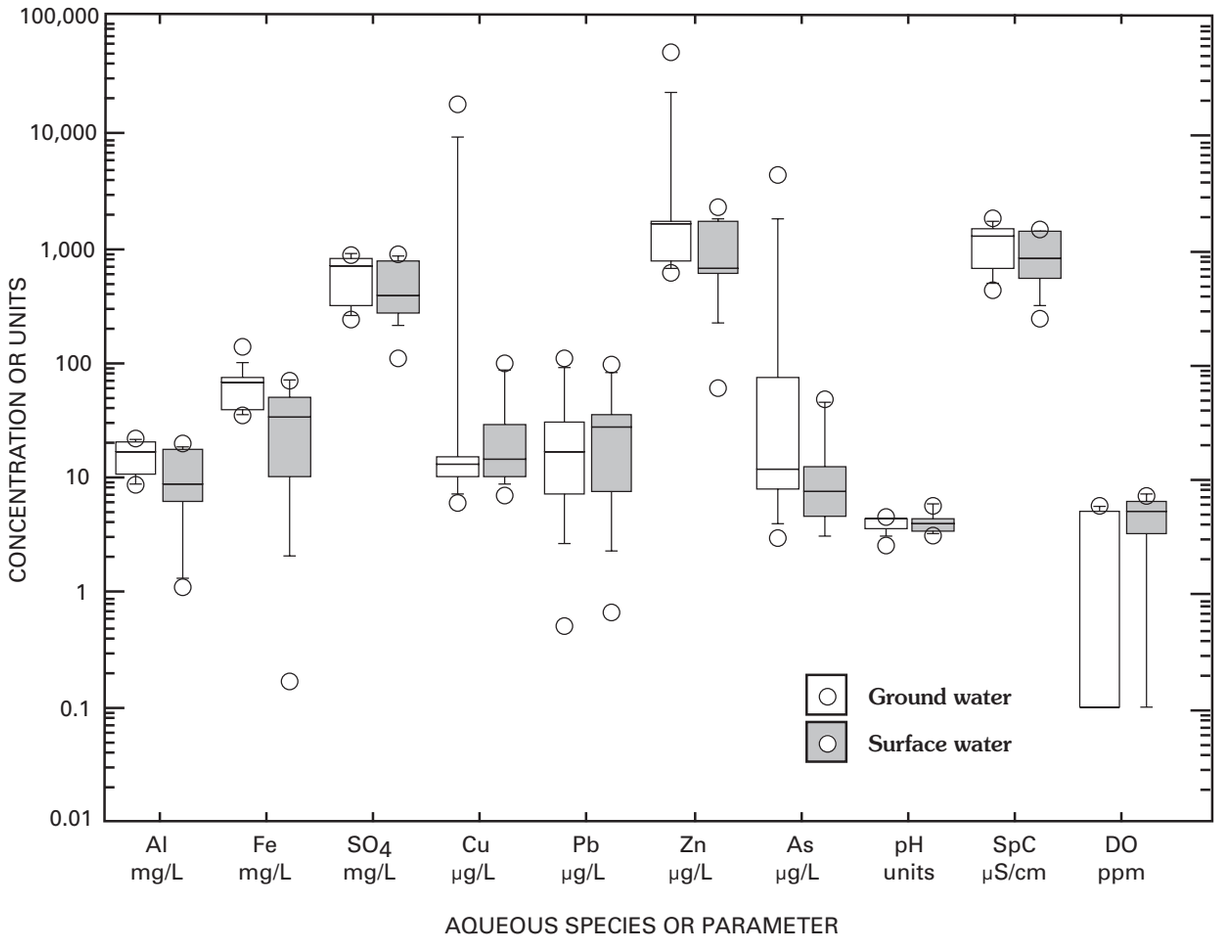

Figure 5. Box plots of major- (mg/L) and trace- (µg/L) element concentrations, and water chemistry parameters in surface and ground water, all iron depositional sites. An arbitrary lower limit of 0.1 ppm DO (dissolved oxygen) has been used for plotting purposes.

Table 5. Summary statistics of major- (Al, Fe, Ca, Si, S (as SO_4), Mn; mg/L) and trace- (Cu, Pb, Zn, As; µg/L) element concentrations, and water chemistry parameters in surface and ground water, all iron depositional sites.

[SpC, specific conductance (µS/cm; microsiemens per centimeter); DO, dissolved oxygen (ppm)]

	Surface water				Ground water			
	n	Minimum	Maximum	Median	*n*	Minimum	Maximum	Median
Al	15	1.1	20.0	8.7	11	8.7	22.1	16.6
Fe	15	0.2	69.8	33.8	11	34.5	140.0	67.2
Ca	15	13	242	111	11	32	280	93
Si	15	7.8	92	27	11	25	78	27
SO_4	15	80	900	390	11	80	910	580
Mn	15	0.2	3.0	1.9	11	0.8	6.2	1.8
Cu	15	2.1	100	14	10	8.0	18,000	13
Pb	13	0.7	100	28	11	0.5	110	16
Zn	15	60	2,300	650	12	630	53,000	1,620
As	13	2	49	7	12	3	4,300	12
pH	15	3.2	5.9	4.0	12	2.7	4.5	4.3
SpC	15	210	1,430	810	12	440	1,900	900
DO	10	0	7.0	5.0	11	0	5.1	0

Surface Water Versus Ground Water—Upper Bog of Cement Creek

The presence or absence of measurable head was a criterion that we used to separate ground water (head present) from surface water (head absent). By this criterion, upper bog surface water shows higher calcium and manganese, identical aluminum and sulfate, and lower iron and silica compared to ground water (fig. 6; table 6). In surface water, median pH is lower while specific conductance and dissolved oxygen are higher.

The similar aluminum and sulfate concentrations in surface and ground water suggest either that both water types arise from a similar source or that the two water types are evolving towards the same composition. Because samples were collected under near-base-flow conditions, ground water and surface water likely originate from the same source. As is evident, iron is the one element that distinguishes ground water from surface water in the upper bog of Cement Creek.

Ratio of Fe^{2+} to Fe_{tot}

For samples where iron species measurements were made, the ratio of Fe^{2+} to Fe^{3+} also proved useful in distinguishing ground water from surface water. Using the separation based on the head measurement, upper bog ground-water samples had high Fe^{2+}/Fe_{tot} ratios, all from 0.98 to 1.0 (table 3), whereas surface-water samples had lower ratios (about 0.95 or less). For example, the lowest ratio from upper bog samples in table 3 was 0.62; this sample also had correspondingly lower total iron. With one exception, when head was not detected (surface water), the highest ratio was 0.94.

Ground and surface water in the immediate vicinity of an active iron bog did not appear to be significantly different with respect to most dissolved elements except iron. This similarity probably reflects multiple ground-water sources of slightly differing composition that emerge and mix in the bog.

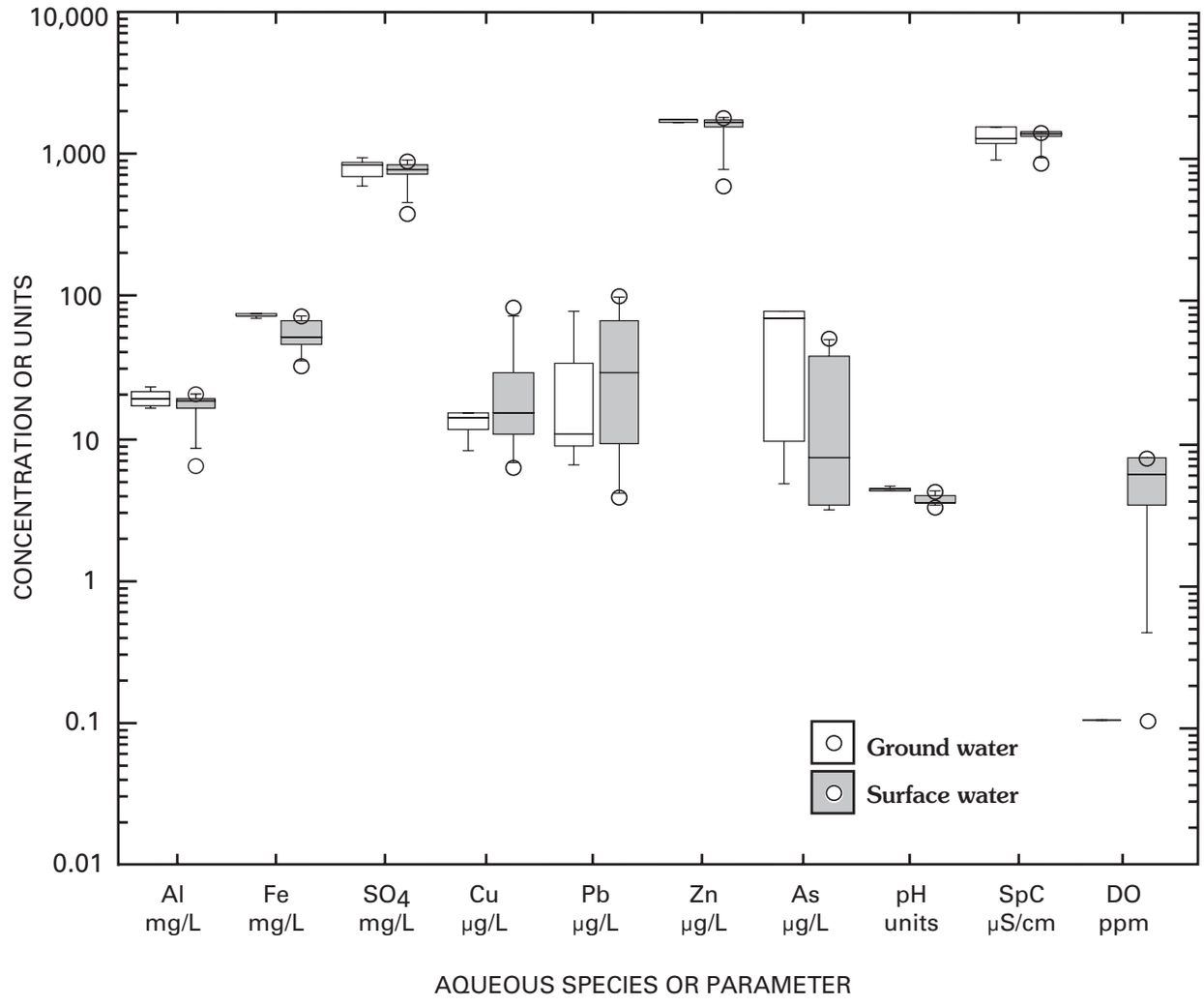

Figure 6. Box plots of major- (mg/L) and trace- (µg/L) element concentrations, and water chemistry parameters in surface and ground water, upper bog of Cement Creek. An arbitrary lower limit of 0.1 ppm DO (dissolved oxygen) has been used for plotting purposes.

Table 6. Summary statistics of major- (Al, Fe, Ca, Si, S (as SO_4), Mn; mg/L) and trace- (Cu, Pb, Zn, As; µg/L) element concentrations, and water chemistry parameters in surface and ground water (based on positive hydraulic head), and nonzero DO and zero DO water, upper bog Cement Creek.

[SpC, specific conductance (µS/cm; microsiemens per centimeter); DO, dissolved oxygen (ppm)]

	Surface water, upper bog				Ground water, upper bog			
	n	Minimum	Maximum	Median	*n*	Minimum	Maximum	Median
Al	6	6.4	20.0	17.6	6	15.0	22.1	17.6
Fe	6	31.8	69.8	51.5	6	42.0	73.2	71.8
Ca	6	102	242	230	6	134	280	221
Si	6	17	27	26	6	25	78	27
SO_4	6	390	900	760	6	580	910	760
Mn	6	1.5	2.4	2.4	6	1.6	2.6	2.2
Cu	6	9.4	82.4	20.4	6	6.0	15	13
Pb	6	3.9	100	30.5	6	4.0	75	9.8
Zn	6	590	1,760	1,670	6	1,500	1,740	1,680
As	6	3.0	49	8.7	6	4.6	77	39
pH	6	3.2	4.2	3.4	6	3.4	4.5	4.2
SpC	6	850	1,430	1,380	6	900	1,520	1,290
DO	5	0	7.0	5.0	5	0	5.8	0

	Other nonzero DO (surface) water				Zero DO (ground) water, upper bog			
	n	Minimum	Maximum	Median	*n*	Minimum	Maximum	Median
Al	19	1.1	20.0	8.8	6	15.9	22.1	18.5
Fe	19	0.2	140.0	35.9	6	50.6	73.2	71.8
Ca	19	23	242	91	6	134.0	280	221
Si	19	7.8	92.0	27.4	6	25.2	27	27
SO_4	19	110	900	350	6	580	910	760
Mn	19	0.2	6.2	1.5	6	1.6	2.6	2.3
Cu	5	9	82	14	6	8.0	28	14
Pb	5	3.9	100	33	6	6.3	75	14
Zn	5	590	1,760	1,630	6	1,620	1,740	1,700
As	5	3.0	49	13	6	4.2	77	39
pH	5	3.2	4.2	3.4	6	3.5	4.5	4.2
SpC	5	850	1,430	1,380	6	900	1,520	1,320
DO	4	0	7.0	6.0	5	0	0	0

Dissolved Oxygen as an Indicator of Ground Water

At the upper bog, the most useful parameter besides iron used to distinguish between ground water and surface water is the dissolved oxygen concentration, especially when "zero" (undetectable) dissolved oxygen was taken as the defining characteristic of ground water. When upper bog water with zero dissolved oxygen (fig. 7*A*; table 6) is compared to surface water from all other sites that are not iron bogs (fig. 7*B*), the narrow ranges of major-element concentrations in iron bog ground water become more evident. Dissolved iron, aluminum, and sulfate in upper bog ground water (zero dissolved oxygen) are present at approximately twice the concentration compared to surface water (nonzero dissolved oxygen) from all other sites.

In ground water, the lack of dissolved oxygen is apparent and pH is higher by about 0.8 units. The higher pH should aid formation of solid iron oxyhydroxides, as these begin precipitating around pH 3.5 (Carlson and Kumpulainen, 2000). Median conductivities are similar, but the higher maximum conductivity of iron bog ground water (based on zero dissolved oxygen) indicates that it contains more solutes than does surface water. The slightly lower maximum conductivity of bog surface water suggests that ground water contains fewer solutes as a result of precipitation of solids containing iron and other species.

When zero dissolved oxygen is used to define ground water, median copper and zinc are at about the same concentration in both water types, whereas lead is about two times lower and arsenic is about three times higher compared to nonzero dissolved oxygen (surface) water (table 6).

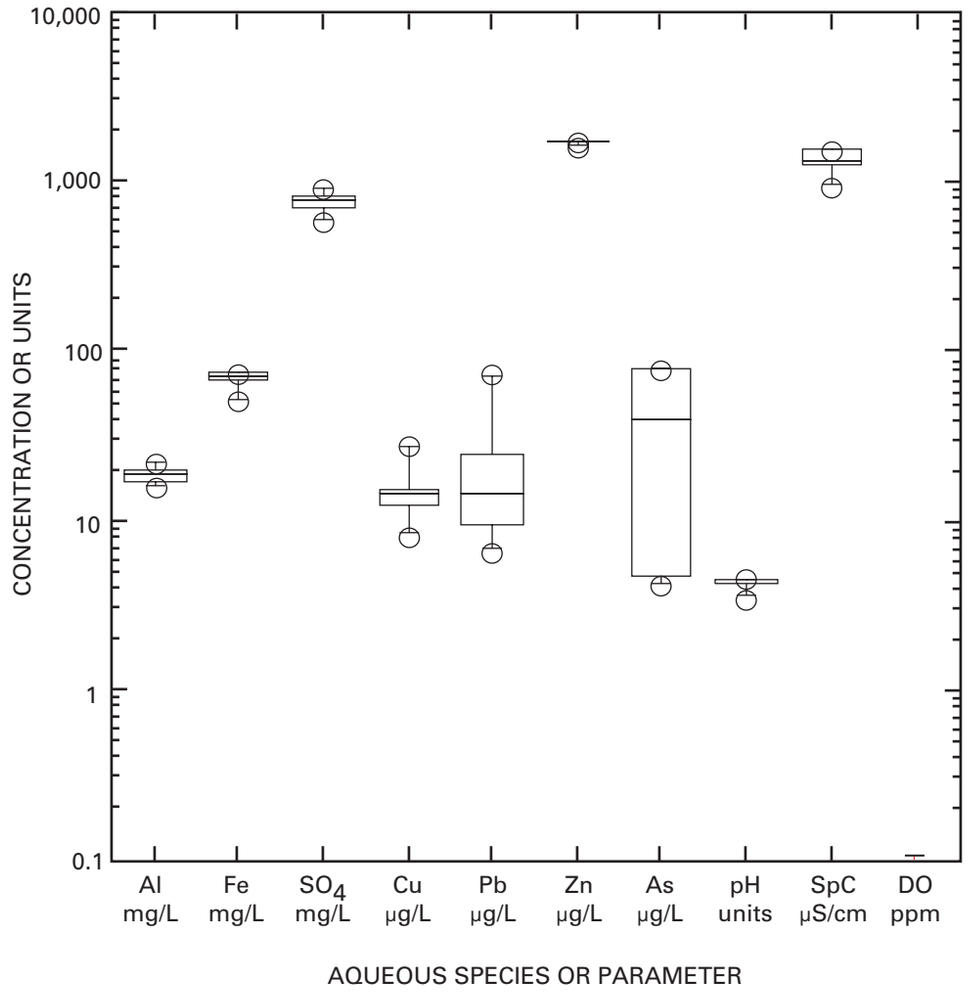

A

Figure 7 (above and facing page). Box plots of major- (mg/L) and trace- (µg/L) element concentrations, and water chemistry parameters in *A*, Zero DO (ground) water, upper bog of Cement Creek, and *B*, Nonzero DO (surface) water from all other sites.

Trace-Element Chemistry and Alteration Type

The common feature of all sites is the presence of iron oxyhydroxide. However, water feeding the iron bogs exhibits wide ranges of aqueous trace-element concentrations (table 3), and the supply of trace elements depends primarily on alteration type drained by ground water.

The Imogene adit (site 5, fig. 1) drains propylitically altered rock, and aqueous trace-metal concentrations are the lowest of all alteration types. Even iron and aluminum are low (both <10 mg/L) compared to water from higher grade alteration types; still, a thin (<5 mm) but areally extensive (6 m by 3 m) iron oxyhydroxide deposit has formed downstream from the outflow.

In contrast, water from acid-sulfate alteration (Junction mine, site 8, fig. 1) shows the highest trace element concentrations (table 3) of all water sampled. At this site, an areally large but thin (100 m^2 by 1 cm) accumulation of iron oxyhydroxide was present. The red spring and upper bog also drain acid-sulfate altered rocks and show correspondingly higher trace element concentrations in both water and sediment. Water draining weak sericite-pyrite and quartz-sericite-pyrite altered areas generally show trace-metal concentrations between these two extremes, in both the aqueous and the solid phases (Bove and others, this volume).

Microbial Populations

The MPN (Most Probable Number) results for eight sites are shown in table 7. Ranges of cell numbers per 100 mL are <2–500 for *Th. ferrooxidans* and <2–440 for *Th. thiooxidans*, calculated according to the formula derived by Thomas (1942). Whereas not all samples produced

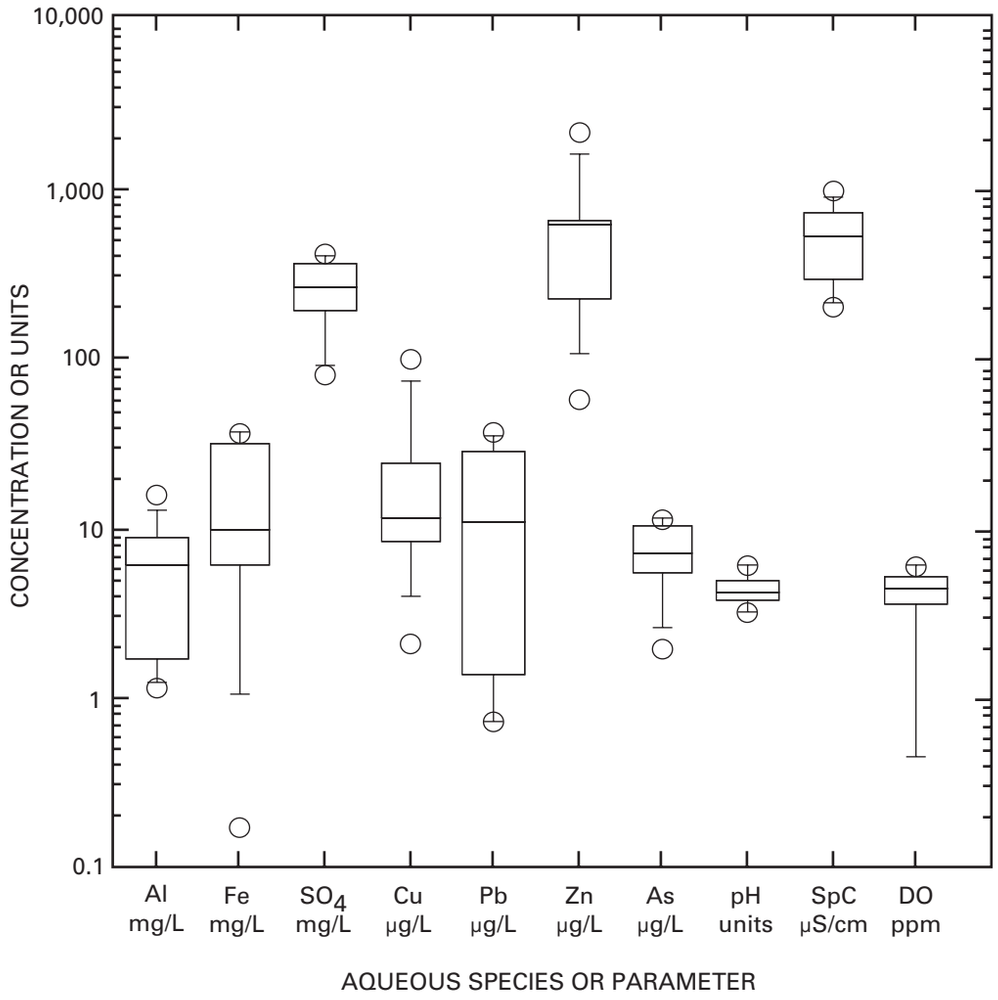

B

Thiobacillus isolates of both species, at least one species and *Leptothrix* sp. were usually present at all iron bogs. The wetland of South Fork Mineral Creek is not an iron bog but is included here to compare *Thiobacillus* numbers from an organic-rich environment versus the iron-dominated sites. There were some positive cultures for *Th. thiooxidans* from the wetland.

The spring deposit in Topeka Gulch showed no positive cultures for either *Thiobacillus* or iron-related bacteria (*Leptothrix)*. This is believed to be the result of our sampling this deposit near the end of a day-long rainstorm, which was preceded by heavy rain the previous day and night. Nearly all chemical concentrations from this site were low, suggesting that this deposit was being flushed by the 2-day rainfall. Because of difficult access to this site, it was not practical to sample again at a later time. Despite the lack of positive cultures, this deposit was similar to other iron deposits with a thick accumulation of iron oxyhydroxide covered by mosses, algae, and cyanobacteria.

One of the more interesting results was the high number of positive cultures (13 of 18 inoculations) at the Junction mine site (site 8, fig. 1). This area receives drainage from a mine adit into a large shallow pool whose bottom surface was covered with iron oxyhydroxide at the time of sampling. The multiple positive cultures may reflect active microbial oxidation of available sulfides inside the mine adit and nearby country rocks.

A contradictory result is the lack of *Th. ferrooxidans* at the upper bog of Cement Creek. Except for the two undiluted inoculations, which showed only slight positive growth, no iron oxidizers were detected. This seems inconsistent with the high percentage of Fe^{2+} in water (≥60 percent of Fe_{tot}), which would appear ideal for promoting growth of

Table 7. Results of Most Probable Number (MPN) culturing for *Thiobacillus* species in iron bogs, Animas River watershed study area.

[Ratings based on relative increase in turbidity of inoculated tubes after 1 month elapsed time, as follows: ---, negative; vs+, very slight positive; s+, slight positive; +, positive. Results shown are for tubes 1–3 (10^{0}–10^{-2}) for each species, as there was no detectable change in tubes at higher dilutions (10^{-3} to 10^{-5})]

Dilution	*Th. ferrooxidans*			*Th. thiooxidans*		
	Tube 1	Tube 2	Tube 3	Tube 1	Tube 2	Tube 3
Junction mine						
10^{0}	+	+	+	s+	s+	s+
10^{-1}	+	+	+	s+	---	---
10^{-2}	+	+	+	---	---	---
Imogene adit						
10^{0}	---	---	+	---	+	---
10^{-1}	s+	s+	---	s+	+	---
10^{-2}	---	+	---	---	---	vs+
Topeka Gulch spring deposit						
10^{0}	---	---	---	---	---	---
10^{-1}	---	---	---	---	---	---
10^{-2}	---	---	---	---	---	---
Bonner mine waste pile						
10^{0}	s+	s+	---	s+	+	s+
10^{-1}	---	s+	s+	---	s+	s+
10^{-2}	---	---	s+	---	---	s+
Iron bog, South Fork Mineral Creek						
10^{0}	---	---	---	s+	s+	---
10^{-1}	---	---	---	---	vs+	vs+
10^{-2}	---	---	---	+	s+	s+
Upper bog, Cement Creek						
10^{0}	vs+	vs+	---	+	+	+
10^{-1}	---	---	---	+	+	+
10^{-2}	---	---	---	---	s+	s+
Wetland, South Fork Mineral Creek						
10^{0}	---	---	---	vs+	+	+
10^{-1}	---	---	---	s+	+	---
10^{-2}	---	---	---	---	s+	---
Red spring, Prospect Gulch						
10^{0}	vs+	---	---	---	---	+
10^{-1}	---	---	---	vs+	---	---
10^{-2}	---	---	---	s+	s+	s+

microbes that prefer Fe^{2+}. Reasons for the lack of iron oxidizers at this site are not readily apparent. One possibility is that *Th. thiooxidans* was able to adapt to act upon iron as well as sulfur, which is a common trait of these chemolithotrophic organisms (Schippers and Sand, 1999).

All iron-related bacteria BART inoculations from active iron bogs produced a (+) result. Color development in some samples required the entire 2-week period. Because the results from the iron-related bacteria tests are nonspecific, the presence of particular iron-oxidizing bacteria cannot be determined. However, the results confirm the presence of one or more microbes whose metabolism is related to iron oxidation and demonstrate that iron-related microbes are present in all iron bogs.

Leptothrix was visible at several sites where pooled water was present and formed an iridescent, oil-like sheen on surface water (fig. 8). Although *Leptothrix* may not actively oxidize iron, it is usually encrusted with a several-micrometer-thick coating of iron oxyhydroxide (an "iron accumulator"), and its presence is considered strongly indicative of active iron oxidation (van Veen and others, 1978).

Geochemical Modeling

Minerals that are saturated or oversaturated in upper bog water (saturation index (SI)>0) include the iron minerals goethite, schwertmannite, and hematite, and the sulfate minerals alunite ($KAl_3(SO_4)_2(OH)_6$) and barite ($BaSO_4$). Of these, goethite and schwertmannite were the dominant iron minerals detected by X-ray diffraction. Jarosite ($KFe_3(SO_4)_2(OH)_6$), a crystalline phase often associated with acid-rock drainage (Bigham and Nordstrom, 2000), was predicted to form in low-pH (<3.0) modeling simulations that did not employ the measured composition of upper bog water. This mineral was detected by X-ray diffraction in only five iron bog samples (table 1; not all jarosite-containing samples are listed). Other sulfate minerals that approach saturation (saturation index (SI) > –1.0 to 0) are gypsum ($CaSO_4 \cdot 2H_2O$), anhydrite ($CaSO_4$), and celestite ($SrSO_4$).

Quartz and chalcedony (amorphous silica) are saturated in the upper bog water. In all iron bogs, few detrital quartz grains were observed macroscopically. Even after visible clasts and grains were removed, quartz was detected as a major phase by X-ray diffraction. The presence of quartz with amorphous silica suggests that most quartz is microcrystalline and newly precipitated within the iron bogs as water moved through the iron oxyhydroxide deposit. This result is consistent with the findings of Desborough and others (2000) that silica gels were forming on filters during filtration of water samples from Cement Creek. In addition, Wirt and others (this volume) found that ferricrete actively forming on the Cement Creek streambed near its boundary with the upper bog was cemented by quartz.

Kaolinite is another aluminosilicate mineral predicted in some modeling simulations, but it is not a stable mineral in acid-sulfate water (Bigham and Nordstrom, 2000). Although detected by X-ray analysis, it is most likely a detrital phase derived from feldspar alteration. Other detrital and secondary silicates identified by X-ray diffraction likely were deposited in the iron bogs by eolian or fluvial processes.

Figure 8. *Leptothrix* film on water surface at lower bog of Cement Creek. Width of pond (from left to right) is approximately 1 meter.

Discussion

Geochemical Evolution of Meteoric and Surface Water to Iron Bog Ground Water

Infiltrating meteoric water can undergo a variety of changes as it evolves to ground water along a flow path (Hem, 1989). Dissolved O_2 is consumed by weathering reactions such as oxidation of sulfide minerals (for example, FeS_2) to form SO_4, which is elevated in ground water. Although ground water has low dissolved oxygen, hydrogen sulfide (H_2S) is not present; thus species such as sulfate form, remain stable, and persist along the flow path (Hanor, 2000). The dominance of Fe^{2+} over Fe^{3+} in upper bog ground water suggests that O_2 is first consumed to oxidize sulfur rather than Fe^{2+}. Bigham and Nordstrom (2000) noted that during pyrite weathering, sulfur in pyrite is oxidized more quickly than iron, producing water enriched in ferrous iron, sulfate, and protons (H^+).

The dominance of Fe^{2+} also suggests that recharge of O_2 to ground water that feeds the iron bogs must be slow or nonexistent. During winter there is little or no infiltration of O_2-bearing surficial water into the subsurface (Vaughn and others, 1999). And because of the acidic nature of the water, Fe^{2+} is only slowly oxidized, if at all, during its residence in ground water. Similarly, iron-oxidizing bacteria are aerobic (requiring oxygen) and not likely to inhabit an O_2-deficient subsurface regime, and therefore, would be unavailable to oxidize iron.

Geochemical Evolution of Iron Bog Ground Water to Iron Bog Surface Water

Ground water discharging into the upper bog shows narrower ranges of dissolved major-element concentrations with higher concentrations (fig. 7*A*; table 3) than surface water. In addition, a lack of dissolved oxygen and higher values for Fe^{2+}/Fe_{tot} ratios (>0.95), Fe_{tot} concentrations, and pH are characteristics that distinguish ground water from surface water at the upper bog.

Surface water exhibits broader ranges of dissolved element concentrations with lower concentrations (fig. 7*B*; table 3) compared to ground water. Surface water has dissolved oxygen greater than zero, and lower values for Fe^{2+}/Fe_{tot} ratios (0.6–0.95), Fe_{tot} concentrations, and pH compared to parent ground water that presumably originated farther up hydrologic gradient.

These observations, including higher median iron and sulfate concentrations in ground water, are all consistent with an oxidation-precipitation process taking place that leads to a lowering of major constituent concentrations in (former) ground water that becomes surface water in the iron bog.

Dilution or mixing of bog water by Cement Creek does not appear to be a likely mechanism for producing the characteristics of the bog surface water. During all sampling periods, Cement Creek was not spilling into the bog, and in fact, has been isolated from the bog by a bench of iron oxyhydroxide (≈25 cm high) that has formed along the bog-stream interface. Physical mixing was limited to the downstream (south) end of the bog where impounded bog water entered the stream.

Several geochemical processes occur during the evolution of the influent bog ground water to bog surface water. The first is oxidation of ferrous iron to ferric iron, which leads to saturation of certain ferric-iron-bearing solids. Second, hydrolysis of oxidized iron and (or) precipitation of ferric iron and sulfate-bearing phases leads to an increase in H^+ in solution (lower pH) and loss of iron and sulfate (and other species) to the solid phase. Finally, the newly evolved bog surface water undergoes precipitation reactions on the bog surface and (or) subsequently farther downstream. The end result is that the characteristics of the influent ground water become altered to those of a surface water. Figure 9 illustrates the evolution of ground water to surface water using data from the upper bog of Cement Creek. A moderate portion (≤40 percent) of the dissolved iron becomes oxidized and potentially sequestered in the solid phase at the bog; some sulfate is also incorporated into the solids when sulfate-bearing phases form.

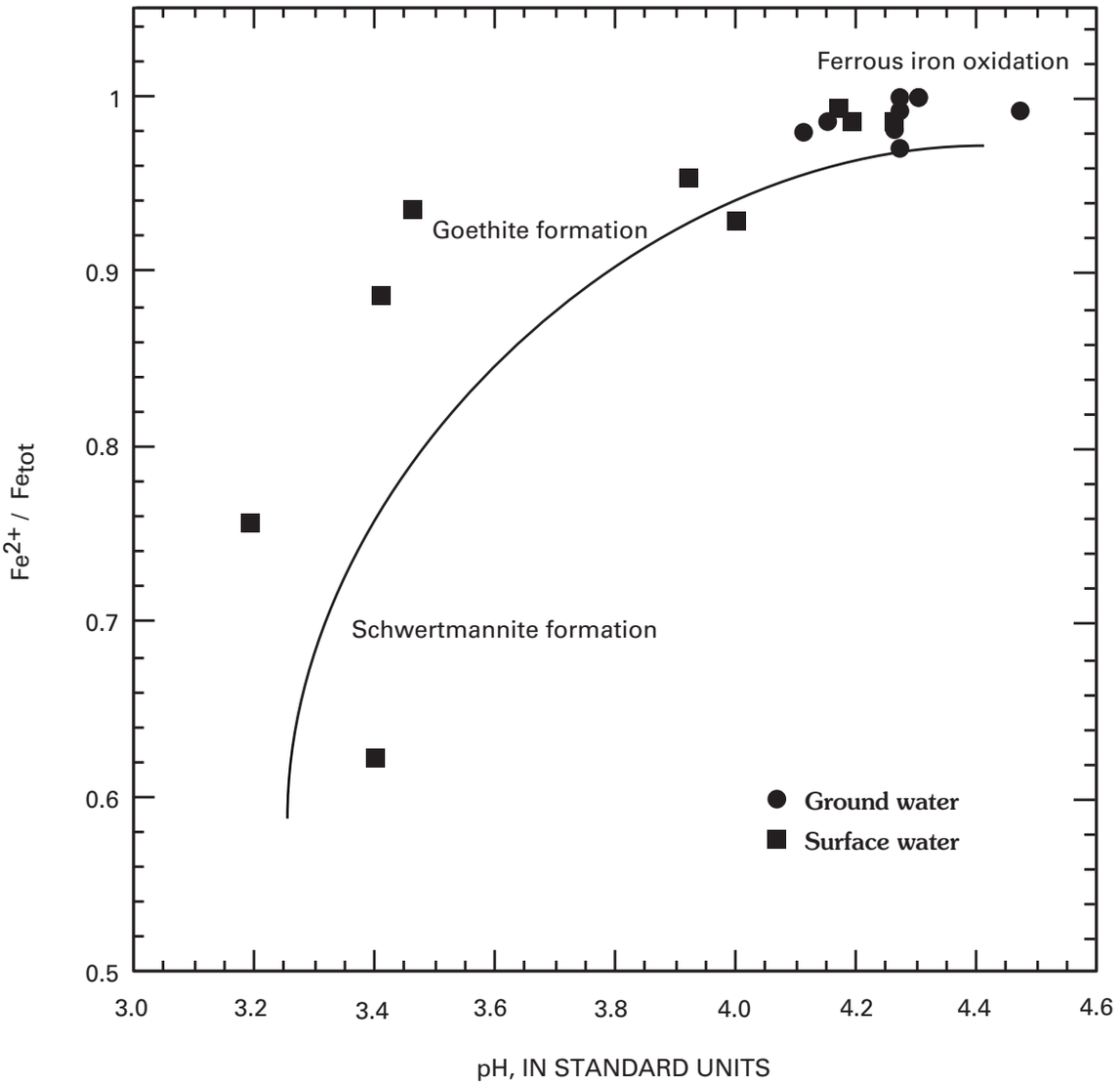

Figure 9. Graph showing postulated evolution of ground water to surface water using data from upper bog of Cement Creek. Note that as bog ground water evolves to bog surface water, both pH and aqueous Fe^{2+} concentration decrease.

Iron Oxidation

Dissolved oxygen in the iron bog originates from the atmosphere and from the activity of photosynthetic plants and microorganisms. Ferrous iron oxidation rendered by atmospheric oxygen or aquatic organisms is a passive process (Canfield and Des Marais, 1993), whereas iron-oxidizing bacteria employ this oxygen to actively accelerate the oxidation. In both the upper bog and the red spring, aquatic plants were heavily encrusted with a light-orange floc of iron oxyhydroxide, indicating that some ferrous iron oxidation occurs near the point of $O_2(g)$ release from the plants. As the floc accumulates on the plant surfaces, portions fall to the bottom of the iron bog to become incorporated into the sediment.

Mosses, cyanobacteria, and algae growing on the bog surface and in small pools and flows were also encrusted with iron oxyhydroxide. All photosynthesizers appear to play dual roles as oxygen producers and thus passive iron oxidizers, and as surfaces to which iron oxyhydroxide can sorb or bind.

The combined high number of positive results from the MPN and IRB tests indicates that microbes are available to act as additional oxidizers of Fe^{2+} in iron bog water. *Thiobacillus* numbers suggest that at mined sites (Junction mine, for example), the populations are relatively higher than in "undisturbed" sites. We surmise that mining has exposed additional fresh pyrite (FeS_2) and other sulfide minerals to oxidation, and that greater numbers of microbes are taking advantage of the available sources of energy (that is, reduced iron and sulfur). Thus, the increase in thiobacilli cell numbers likely mirrors the increased availability of reduced forms of iron and sulfur and increased oxidation mediated by the microbes. The presence of *Leptothrix* at most sites (fig. 8) was indicative of active, ongoing iron oxidation. Although microbial oxidation of Fe^{2+} was not directly observed in our study, that iron and sulfur oxidizing microbes inhabit the iron-depositing environments is likely because of the plentiful supply of energy-yielding reduced iron and (perhaps) sulfur.

Formation of Iron Oxyhydroxide and Schwertmannite

Despite variability in water composition at different iron-depositing sites, all water becomes saturated with respect to iron oxyhydroxide; the mechanism that leads to initial saturation is oxidation of Fe^{2+} to Fe^{3+}. Once this occurs, ferrihydrite, goethite, and schwertmannite may precipitate from solution, depending on the solubility (saturation state) of each mineral, redox potential (approximated by dissolved oxygen concentration), and pH. Modeling indicated that slight changes over the pH range 4.0–4.5 can affect which of the three solids will form. As ground water undergoes these precipitation reactions, it acquires more of the surface water characteristics, the most important being more-acidic pH via production of hydrogen ion (H^+).

One process that could reduce pH to more-acidic values is the oxidation of ferrous iron to ferric iron followed by hydrolysis to form ferrihydrite:

$$Fe^{3+} + 3H_2O \rightarrow Fe(OH)_3 + 3H^+ \quad (1)$$

The formula for ferrihydrite is considered uncertain (Bigham and Nordstrom, 2000); ferrihydrite may consist of both crystalline and amorphous material depending on conditions at the time of formation. Protons (H^+) are generated in solution and iron is removed as $Fe(OH)_3$ drops out as a solid. As there is little or no acid-neutralizing capacity in the water, it continues to evolve towards bog surface water with lower pH and lower concentrations of total and ferrous iron. At the iron and sulfate concentrations and slightly higher pH (>4.0) of some upper bog ground-water samples, goethite would be the preferred phase (Carlson and Kumpulainen, 2000).

$$Fe^{3+} + 2H_2O \rightarrow FeOOH + 3H^+ \quad (2)$$

The Eh-pH diagram of Bigham and others (1996) shows that increasingly positive redox potentials at low pH (<4.5) favor formation of schwertmannite over goethite. As bog ground water evolves to bog surface water, the increase in dissolved oxygen concentration coupled with production of H^+ via ferric iron hydrolysis or goethite formation could lower pH and favor formation of schwertmannite.

$$8Fe^{3+} + SO_4^{2-} + 14H_2O \rightarrow Fe_8O_8(OH)_6SO_4 + 22H^+ \quad (3)$$

The upper bog of Cement Creek displays a variety of redox potentials, a range of pH values (3.19–4.47) that encompasses the stability fields of schwertmannite (pH 3.0–4.5) and goethite (pH 3.5–8.0) (Bigham and others, 1996; Bigham and Nordstrom, 2000), and varying iron and sulfate concentrations. It is these differing geochemical conditions that allow both iron minerals to form. Schwertmannite can convert to goethite via the reaction:

$$Fe_8O_8(OH)_6SO_4 + 2H_2O \rightarrow 8FeOOH + 2H^+ + SO_4^{2-} \quad (4)$$

The release of sulfate in this conversion may be the reason why iron bog ground water and surface water do not differ greatly with respect to sulfate concentrations (table 4), whereas iron concentrations vary more because all minerals that form consume iron.

The formation of other sulfate minerals such as jarosite, which was predicted to precipitate in some modeling simulations, would also cause decreased SO_4 in water that becomes surface water. Barite, which was predicted by modeling but not detected by X-ray diffraction, could potentially form. However, it would not change the pH as there is no production or consumption of protons.

$$(Ba^{2+} + SO_4^{2-} \rightarrow BaSO_4) \quad (5)$$

In summary, acidity is generated by precipitation of iron sulfate minerals such as schwertmannite and iron minerals such as goethite. These precipitation reactions are key processes that produce and maintain the acid character of iron bog surface water.

Mineralogy of Iron Bog Solids

Goethite and schwertmannite are the most abundant iron-bearing minerals in iron bog solids (table 1). The presence of schwertmannite at depth in the iron bogs suggests that there are kinetic or thermodynamic factors that permit this mineral to persist as a metastable form rather than convert to goethite. In contrast, fresh schwertmannite precipitates that formed early in the summer in stream beds and on the surfaces of several iron bogs (Desborough and others, 2000) did not persist year-round. Schwertmannite was not detected later in the fall in most streams, so these precipitates apparently dissolved (or perhaps were transformed to goethite) when water levels in the streams dropped (Desborough and others, 2000). These results suggest differing stabilities of schwertmannite and goethite in iron bogs compared to open areas such as streams.

Bigham and others (1990) reported that schwertmannite is the preferred iron phase to form at pH 3.5–4.0 in acid-sulfate water (similar in composition to that at the upper bog of Cement Creek). At slightly higher pH (>4.0) or sulfate concentration (as high as 1,000 mg/L), goethite is favored over schwertmannite. Carlson and Kumpulainen (2000) noted that if iron is oxidized by *Thiobacillus* rather than molecular oxygen, schwertmannite is the dominant solid phase that forms. Assuming the aqueous chemistry varies temporally (daily to seasonally), then to expect both phases to be produced in the iron bogs is not unreasonable.

The iron bog mineralogy is in agreement with the predicted (by modeling) crystalline solids. That is, goethite and schwermannnite were predicted as the main crystalline iron-bearing phases and were observed. Hematite was predicted to form as it is the stable (equilibrium) iron mineral, but it was not present in the iron bogs. Goethite may transform to hematite under some conditions, but most research suggests that "coarse-grained" goethite (>1 μm size) is kinetically stable to hematite at below-neutral pH values (Fischer and Schwertmann, 1975). Given the highly acid pH values in the iron bogs, hematite is not likely to form via the dehydration and aging of goethite.

Goethite and hematite form from a common ferrihydrite precursor but along separate pathways, and kinetics and pH are major controls on which phase actually forms and remains stable (Fischer and Schwertmann, 1975). The rate of aggregation of (amorphous) ferrihydrite particles seems especially important in controlling which iron mineral initially forms. Hematite formation requires rapid aggregation of ferrihydrite followed by hematite crystallization and aging at higher pH (7–8), whereas goethite forms when ferrihydrite aggregation is slow. Dissolution of the ferrihydrite precursor and precipitation of goethite will be dominant at low pH (Fischer and Schwertmann, 1975).

Additionally, laboratory studies indicate the goethite-hematite conversion to be extremely slow, requiring years under optimal conditions to perhaps thousands of years under non-ideal conditions (Langmuir and Whittemore, 1971). The bog deposits are geologically young, having formed in approximately the last 9,000 years, and most are still active, so the extremely slow conversion process (that is, attainment of equilibrium) has not occurred.

Jarosite forms at lower pH values (<3.0; Bigham and others, 1996) and was detected in only five samples, so it appears that only rarely did pH permit jarosite precipitation. Barite precipitation might be occurring near the ground water–surface water interface, as indicated by lower dissolved barium in ground water compared to surface water, but barite was not detected as a solid phase by X-ray analysis.

Location of Precipitation of Solid Phases

Newly evolved surface water moves onto the bog surface where residual ferrous iron can undergo oxidation. Because the water is now at a lower pH and higher redox potential, schwertmannite is the preferred phase to precipitate. This may explain why fresh precipitates on bog surfaces are dominantly schwertmannite rather than goethite.

Field observation indicates that some iron precipitation happens within the region between the shallow bottom surface, close to the point of ground-water discharge, and the top surface of growing bogs that contain pooled water. Iron bogs appear to reconstitute from the interior and below water level after their surfaces have been penetrated or disrupted by sampling, rather than by deposition from the surface downward.

The geochemical modeling results also suggest that the iron deposits accumulate, at least partially, from the bog interior (or bottom) towards the surface. The models indicate that changes in water chemistry and formation of solid iron oxyhydroxide occur at the point of ground-water discharge at the base of the bog. However, because of additional mixing and iron oxidation after ground-water discharge into the iron bog, it is not possible to determine the precise location(s) where iron precipitates from solution.

The presence of >60 percent ferrous iron in all upper bog water samples indicates that most Fe^{2+} delivered by ground water passes through the site and continues downstream in Cement Creek to be oxidized and precipitated. Kimball and others (this volume, Chapter E9) noted that the Prospect Gulch–upper bog area was a major contributor to the metal load of Cement Creek. The lack of complete oxidation at the bog site results in a source of ferrous iron to the stream and helps explain the presence of fresh silica-bearing schwertmannite precipitates (Desborough and others, 2000) in streambed reaches where ground-water inflow was not observed.

Solid Phase Chemistry Versus Alteration Type

Trace-Element Composition of Iron Oxyhydroxide

Trace-element concentrations in iron bog sediment show broad ranges that are affected primarily by the type of alteration and mineralogy of the terrain drained by ground water. Bove and others (this volume) found distinct aqueous geochemical signatures originating from each alteration type.

Water draining the propylitic alteration type (Imogene adit, site 5, fig. 1) contains among the lowest dissolved major- and trace-element concentrations of all water samples. By contrast, water from the Junction mine acid-sulfate site (site 8, fig. 1) shows remarkably high dissolved element concentrations, including 4,300 mg/L arsenic. The site of core 97ABS327 (site 13, fig. 1; located 0.6 km east and 700 m downslope from the Junction mine) drains this same acid-sulfate zone, and solid-phase arsenic is at the highest level of any of the iron bogs. The higher dissolved arsenic in zero dissolved oxygen upper bog water (which also drains the acid-sulfate zone) can be explained by the fact that under mildly reducing conditions, the reduced form of arsenic [As(III)] is generally the more mobile and more soluble species (Smedley and Kinniburgh, 2002). In the iron bog sediment, arsenic becomes strongly associated with iron oxyhydroxide through oxidation to As(V) and coprecipitation with ferric iron (Smedley and Kinniburgh, 2002).

Copper is present in the iron sediment from the site of core 97ABS327 (site 13, fig. 1; red spring), yet the aqueous sample did not show detectable copper. In the interval from approximately 10 to 30 cm (fig. 3), copper was elevated (to as high as 70 ppm) compared to other intervals. This suggests either episodic contribution and retention of copper from ground water or continued accumulation of minute levels of copper through time.

Lead had the lowest maximum concentration in the solid phase. Normalization of other element data to the lead concentration produces the following "enrichment" factors in core 97ABS327: Fe = 7,500×; Cu=1.2×; Pb = 1×; Zn = 11×; As = 83×. These values indicate that large amounts of iron oxyhydroxide must be precipitated to retain small amounts of trace elements. The relatively low copper, lead, and zinc values are likely the result of reduced adsorption and (or) coprecipitation of these metals with iron oxyhydroxide at low pH (Zanker and others, 2002), whereas arsenic is more strongly adsorbed (Smedley and Kinniburgh, 2002).

In contrast to core 97ABS327, solids from core 999291 (site 11, fig. 1) show low but consistent copper concentrations of 10–30 ppm throughout the core; and in fact, copper is detectable in all but two samples. This site, located on the southern flanks of the subeconomic copper moly-porphyry deposit at peak 3,792 m, receives ground water from higher slopes. Although the drainage area is dominantly unmineralized propylitically altered Paleozoic sedimentary rocks and quartz-sericite-pyrite altered rocks with low abundances of deposit-related trace elements such as arsenic and lead, the influence of ground water from the peak's WSP alteration suite is reflected in the composition of the iron bog sediment.

The modern iron oxyhydroxide cement from the Bonner waste pile (site 6, fig. 1) has little or no aluminum in the solid phase, but substantial trace-element concentrations compared to those of iron bog solids. This mine waste ferricrete thus appears to be capable of retaining most of the same elements as iron bogs with the exception of aluminum. The most likely reason that aluminum is not retained in these solids is that the pH of ground water (exiting the adit) was one of the lowest measured (3.17). At low pH, aluminum is a conservative species that remains in the aqueous phase and does not precipitate.

Water Chemistry Versus Alteration Type

Water samples from each environment that we examined show differing concentrations of iron and aluminum that reflect combined influences of local rock type (mineralogy), alteration type, and depositional conditions. Water falls into four major groups identifiable by iron and aluminum concentrations and depositional environment (fig. 10). Iron bogs contain the highest aqueous iron and aluminum compared to water from other iron-depositing environments (fig. 10; table 4). Seeps are intermediate in composition, having approximately 30–40 mg/L iron but lower aluminum, 5–10 mg/L (fig. 10). Even more dilute is surface water (including the Imogene and Bonner drainages, and Mineral Creek and Topeka Gulch springs), which does not exceed about 10 mg/L iron and 5 mg/L aluminum (fig. 10). The fourth group (not shown in fig. 10) is made up of water from wetlands primarily along South Fork Mineral Creek. These show the lowest aqueous concentrations, generally less than 10 mg/L iron and 5 mg/L aluminum (Stanton, Fey, and others, this volume). The low values in wetlands may partly reflect the ability of these systems to remove dissolved species from influent water through adsorption onto organic matter or precipitation of authigenic minerals such as metal sulfides. However, the low iron and aluminum concentrations most likely reflect the lack of intense alteration and sustainable acidic weathering of the Paleozoic sedimentary rocks in the South Fork Mineral Creek drainage.

Iron bogs represent environments where acid weathering has allowed accumulation of high concentrations of dissolved iron, aluminum, and trace elements along the ground-water flow path. Many of these elements become fixed in the solid iron oxyhydroxide sediment that forms as a result of geochemical changes at the depositional site. Thus, iron bogs are sites of deposition that display the end result of deep, intense weathering in the rocks. In contrast, the lower concentrations of aqueous iron and aluminum in the other depositional environments (seeps, springs, adits) suggest either that weathering is less intense or complete, or that depositional conditions are not as favorable for production and preservation of large accumulations of iron-rich solids.

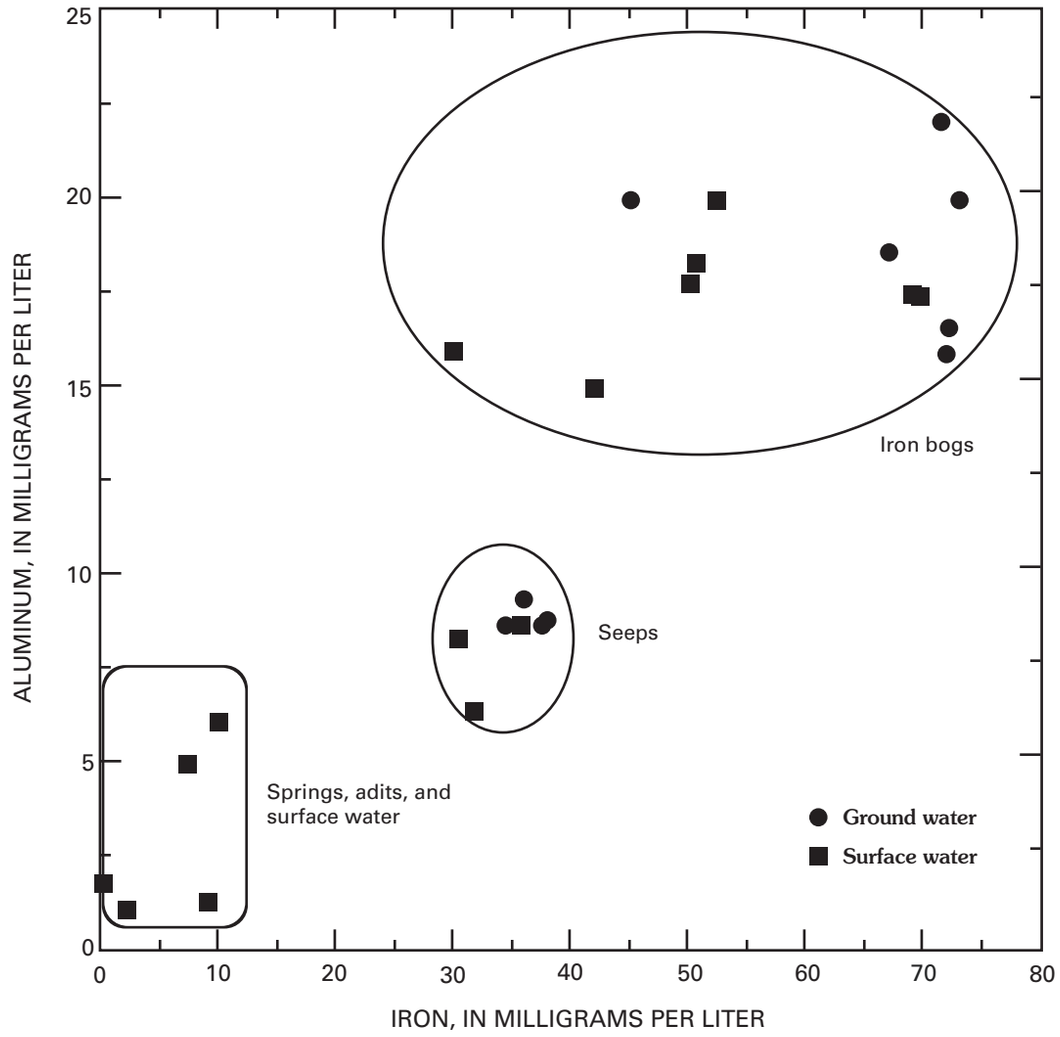

Figure 10. Relationship of aqueous concentrations of iron and aluminum in all iron depositional environments.

Accumulation of Iron Oxyhydroxide

Formation of Modern "Waste-Pile Ferricrete" Deposits

The formation of iron oxyhydroxide cement in iron-rich rocks can be rapid with respect to geologic time, on the order of 50 to 100 years. This is evidenced by the presence of iron-cemented "anthropogenic" deposits in several mine-waste rock piles in the area.

At the Yukon tunnel on Cement Creek (site 17, fig. 1), a large block of mine-waste material has been iron-cemented and differentially weathered so that the ferricrete now stands out in relief against the rest of the surrounding pile. The earliest mining in the region began in the 1870s. The Yukon operations began around 1900 and continued intermittently until around 1950 when the mine became inactive (San Juan Historical Society Archives, 1998); succeeding decades saw only occasional activity.

Similarly, another waste-pile ferricrete was observed on the Bonner mine waste pile (site 6, fig. 1). (This pile has since been remediated so the ferricrete no longer exists.) The relationship of water flow to the location of this ferricrete was clear. Water originating in the upper levels of the pile flowed underground and down into the waste pile, then resurfaced along an old roadbed in the middle of the pile; a 6 m long by 1 m thick section of this roadbed had been cemented by iron oxyhydroxide. The Bonner mine began operations around 1910 and ceased in 1955 (San Juan Historical Society Archives, 1998). Thus, in a span of about 50 years, a small deposit of ferricrete formed.

Approximately 50 vertical feet downhill from the roadbed ferricrete, the area surrounding a flowing adit had also been cemented by iron oxyhydroxide. This deposit was well indurated and similar in hardness to ferricrete cement, but contained few clasts and was dominantly fine grained iron oxyhydroxide. The adit appeared to flow perennially, allowing it to deposit a large volume and thickness of iron oxyhydroxide

around the adit discharge area. Below the adit discharge was a level bench of waste rock that was now encrusted with several centimeters of fine-grained iron oxyhydroxide and covered with living mosses, very similar in appearance to a typical bog such as the lower bog of Cement Creek (fig. 2).

Mine adit drainages are another location where small iron deposits have formed in recent times. Near the Imogene adit, a thin (≤2 mm) but areally extensive (10 m by 2 m) homogeneous accumulation of fine-grained iron oxyhydroxide had formed across a dirt road downstream of the flowing adit. However, this layer was ephemeral—on a return visit to this site 8 months after the first encounter, most of the iron oxyhydroxide layer had dissolved. But 3 m downstream on a slope (4 m high) just below the road level, the iron oxyhydroxide accumulation was 2–4 cm thick. Once again, the solids were retained among a thick growth of photosynthetic macroorganisms. The situation at this adit illustrates that even on a local scale, some areas are more favorable for the permanent accumulation of iron oxyhydroxide than others.

Below the Junction mine on Mineral Creek, a layer of iron oxyhydroxide several millimeters thick accumulated in just a few years since the site was remediated, and an incipient iron bog was being established. Near the Cascade Gulch adit, iron oxyhydroxide (fig. 11) nearly 1 m thick has accumulated; it has taken no longer than 130 years for this thick deposit to form. Similarly, much of the east upper bog (20 m east of the upper bog of Cement Creek, site 4, fig. 1) has been deposited since railroad ties were first placed there in the late 1890s, as evidenced by the ties being encrusted and partially buried with several centimeters of iron oxyhydroxide. Thus, in a span of time ranging from about 50 to 130 years, several "modern" iron deposits have formed.

These more recent iron deposits are able to form rapidly because the higher porosity of the angular cobbles and boulders (compared to competent country rock) enhances surface-water percolation and ground-water flow through the waste pile. The supply of ferrous iron is likely increased because of the greater available surface area of the crushed waste metal-bearing sulfides. The larger surface area enhances the rate of Fe^{2+} solubilization and delivery to the depositional site (for example, the bottom of the Bonner waste pile), which in turn helps to accelerate iron cement formation. In contrast, natural iron bogs are limited by slower processes of recharge, ground-water movement, weathering (smaller mineral surface areas for dissolution), iron solubilization, and iron delivery to the depositional site.

Role of Photosynthetic Organisms

As shown in figures 2, 8, and 11, plants, mosses, algae, and cyanobacteria are abundant in and on the iron bogs. In every instance, one or more of these organisms was found in active iron bogs. Mosses in particular appear to stabilize the growth and accumulation of the bog through retention of iron oxyhydroxide precipitate.

The Cascade Gulch adit on Cement Creek (site 15, fig. 1) provided some insight into the role of organisms in the accumulation of iron. Here, both mosses and algae were growing in

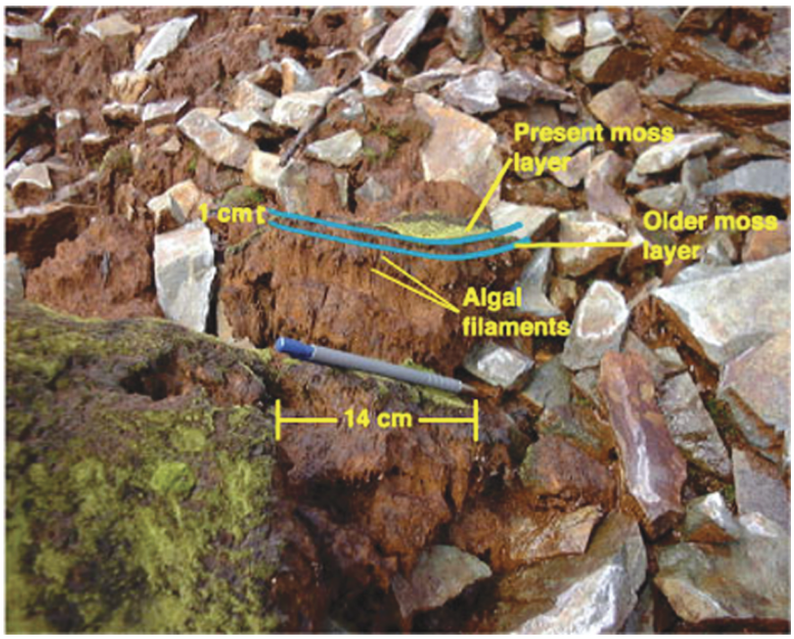

Figure 11. Moss layer (bright green) and relict algal filaments (vertical thin black strands) enclosing a 1-cm thick layer of iron oxyhydroxide near Cascade Gulch adit, Cement Creek. The layer has slumped and broken apart, but moss was once continuous across a thick layer of iron oxyhydroxide.

the iron deposit and acted to retain and stabilize the accumulating sediment. Figure 11 illustrates a vertical sequence of fresh and relict moss layers and algal strands enclosing a 1-cm thick layer of iron oxyhydroxide that accumulated during (one or more) growing seasons. In deeper (older) layers of some iron bogs, it was clearly evident that relict mosses were in the process of being replaced by iron oxyhydroxide.

Cyanobacteria and algae were seen on the surfaces of most active bogs, with distinct cyanobacteria layers alternating with iron oxyhydroxide layers in the upper core samples of all large iron bogs. This is likely the result of one season's growth of cyanobacteria and algae, which are subsequently covered by the iron oxyhydroxide that precipitates during the following season(s). These layers are not well preserved in deeper parts of the iron bog, presumably owing to advancing (but incomplete) oxidation and destruction of organic matter as the material gets older. Nonetheless, iron-oxyhydroxide-replaced structures resembling fine algal or cyanobacterial filaments were seen in the deeper layers of several inactive and active bogs.

Estimated Rates of Iron Oxyhydroxide Deposition

Samples from two iron bogs on South Fork Mineral Creek provide a rough estimate of the rate of accumulation of iron oxyhydroxide in that drainage. Sample 97ABS319, a peat from a depth of 20.3 cm in an iron bog, produced a ^{14}C age of 1,480(±40) yr B.P. Assuming a constant rate of iron oxyhydroxide deposition with no removal through erosion or dissolution, an estimated accumulation rate of 0.13 m/1,000 years is obtained. Similarly, peat sample 97ABS320 from a depth of 30.5 cm in another iron bog had a ^{14}C age of 1,920(±190) yr B.P., or an accumulation rate of 0.16 m/1,000 years. The thickness of iron bogs in the Animas River watershed study area ranges from about 1 to 2 meters. At the higher depositional rate, it would require about 6,250 years to deposit a 1-m thick layer of iron oxyhydroxide. This estimated rate falls within the time range delimited by ^{14}C dates, which show that the iron deposits (including ferricrete) formed within approximately the past 9,000 years (Vincent and others, this volume).

Although the ^{14}C dates provide only a minimum age of deposition, they do show that the iron deposits have formed since the last glaciation in the area (Hanshaw, 1974). This seems a reasonable result because it is unlikely that the iron deposits could form when stream beds and valleys were occupied by ice, and both glacial action and subsequent erosion may have removed previous iron accumulations.

Although these depositional/accumulation rate estimates are imprecise, they help to illustrate that iron bog growth is indeed a slow process. Other factors can strongly affect the depositional rate in individual iron bogs, such as migrating ground-water flow paths, episodic or cyclical changes in precipitation and ground-water discharge, and variations in the rate of iron supply (weathering) and oxidation. The large spring deposit on Mineral Creek (site 10) may be an example of episodic deposition. Currently, surface discharges of ground water are small and isolated, but in the past, ground-water flow and iron deposition likely were much higher to produce this thick, widespread accumulation of iron oxyhydroxide. In contrast to the estimated accumulation rates in South Fork Mineral Creek, the large Iron Springs deposit on the west side of the basin divide (west of Ophir Pass) had a relatively rapid accumulation rate of 0.9 m/1,000 years (Hanshaw, 1974).

Carbon Preservation within Iron Bogs

To have found relict organic carbon in the iron bogs is noteworthy because these bogs are oxidizing environments. The dominance of Fe^{3+} in the solids suggests that any organic matter should be completely oxidized and not preserved. However, as noted previously, much of the aqueous reduced Fe^{2+} remains in that state and is not immediately nor completely oxidized to Fe^{3+}. As a result of the slow, incomplete oxidation of the pool of ferrous iron and therefore deposition of iron oxyhydroxide, the iron bogs have slow growth and accumulation, which is further evidenced by the ^{14}C ages of many of the deposits.

The reduction of dissolved oxygen to zero values by high aqueous Fe^{2+} is one reason that organic carbon is able to survive. Preservation of organic matter within these geologically young systems is possible—and is occurring. Relict organic carbon was readily visible in the upper iron oxyhydroxide layers of active iron bogs but not macroscopically visible in deeper layers.

Delivery of Fe^{2+} and oxidation to Fe^{3+} are processes that can occur at differing rates and would depend on factors such as ground-water flow rates, diffusion of O_2 into bog water, or microbial kinetics. Diurnal effects were not examined but could be important, as daytime iron oxidation rates may be four times greater than at nighttime (McKnight and others, 1988). Thus, accumulation of iron bog solids may be limited by processes that occur during specific periods of the day or seasons of the year.

References Cited

Allison, J.D., Brown, D.S., and Novo-Gradac, K.J., 1991, MINTEQA2/PRODEFA2, a geochemical assessment model for environmental systems, ver. 3.0 user's manual: U.S. Environmental Protection Agency, EPA/600/3–91/021.

Atlas, R.M., 1995, Handbook of media for environmental microbiology: Boca Raton, Fla., CRC Press, 540 p.

Bigham, J.M., 1994, Mineralogy of ochre deposits formed by sulfide oxidation, *in* Jambor, J.L., and Blowes, D.W., eds., Environmental geochemistry of sulfide mine-wastes: Mineralogical Society of Canada, p. 103–132.

Bigham, J.M., and Nordstrom, D.K., 2000, Iron and aluminum hydroxysulfates from acid sulfate waters, *in* Sulfate minerals—Crystallography, geochemistry, and environmental significance: Mineralogical Society of America Reviews in Mineralogy and Geochemistry, v. 40, p. 351–403.

Bigham, J.M., Schwertmann, U., Carlson, L., and Murad, E., 1990, A poorly crystallized oxyhydroxysulfate of iron formed by bacterial oxidation of Fe(II) in acid mine waters: Geochimica et Cosmochimica Acta, v. 54, p. 2743–2758.

Bigham, J.M., Schwertmann, U., Traina, S.J., Winland, R.L., and Wolf, M., 1996, Schwertmannite and the chemical modeling of iron in acid sulfate waters: Geochimica et Cosmochimica Acta, v. 60, p. 2111–2121.

Briggs, P.H., 2002, The determination of forty elements in geological and botanical samples by inductively coupled plasma–atomic emission spectrometry, Chapter F *in* Taggart, J.E., Jr., ed., Analytical methods for chemical analysis of geologic and other materials: U.S. Geological Survey Open-File Report 02–223, p. F1–F11.

Brown, Z.A., and Curry, K.J., 2002, Total carbon by combustion, Chapter R *in* Taggart, J.E., Jr., ed., Analytical methods for chemical analysis of geologic and other materials: U.S. Geological Survey Open-File Report 02–223, p. R1–R4.

Canfield, D.E., and Des Marais, D.J., 1993, Biogeochemical cycles of carbon, sulfur, and free oxygen in a microbial mat: Geochimica et Cosmochimica Acta, v. 57, p. 3971–3984.

Carlson, L., and Kumpulainen, S., 2000, Mineralogy of precipitates formed from mine effluents in Finland, *in* Proceedings of the 7th International Conference on Tailings and Mine Waste, Ft. Collins, Colo., January 1999: Rotterdam, Netherlands, Balkema, p. 269–275.

Church, S.E., Kimball, B.A., Fey, D.L., Ferderer, D.A., Yager, T.J., and Vaughn, R.B., 1997, Source, transport, and partitioning of metals between water, colloids, and bed sediments of the Animas River, Colorado: U.S. Geological Survey Open-File Report 97–151, 135 p.

Curry, K.J., 1990, Determination of total carbon in geologic materials by combustion, *in* Arbogast, B.F., ed., Quality assurance manual for the Branch of Geochemistry, U.S. Geological Survey: U.S. Geological Survey Open-File Report 90–668, p. 114–118.

Desborough, G.A., Leinz, R.W., Smith, K.S., Hageman, P.L., Fey, D.L., and Nash, T.J., 1999, Acid generation and metal mobility of some metal-mining related wastes in Colorado: U.S. Geological Survey Open-File Report 99–322, 18 p.

Desborough, G.A., Leinz, R.W., Sutley, S.J., Briggs, P.H., Swayze, G.A., Smith, K.S., and Breit, G.N., 2000, Leaching studies of schwertmannite-rich precipitates from the Animas River headwaters, Colorado and Boulder River headwaters, Montana: U.S. Geological Survey Open-File Report 00–0004, 16 p.

Fischer, W.R., and Schwertmann, U., 1975, The formation of hematite from amorphous iron(III) hydroxide: Clays and Clay Mineralogy, v. 23, p. 33–37.

Gerhardt, P., Murray, R.G.E., Wood, W.A., and Krieg, N.R., eds., 1994, Methods for general and molecular bacteriology: American Society Microbiology, Washington, D.C., 791 p.

Gore, A.J.P., 1983, Mires—Swamp, bog, fen, and moor; regional studies, *in* Goodall, D.W., ed., Ecosystems of the world 4B: Amsterdam, Netherlands, Elsevier, 479 p.

Hach Company, 1996, Procedures Manual for DR/2010 Spectrophotometer: Loveland, Colo., 824 p.

Hanor, J.S., 2000, Barite-celestine geochemistry and environments of formation, *in* Sulfate minerals—Crystallography, geochemistry, and environmental significance: Mineralogical Society of America Reviews in Mineralogy and Geochemistry, v. 40, p. 193–275.

Hanshaw, Bruce, 1974, Geochemical evolution of a goethite deposit, *in* Proceedings of the 1st International Symposium on Water-Rock Interaction, Prague, Czechoslovakia: p. 70–75.

Hem, J.D., 1989, Study and interpretation of the chemical characteristics of natural water: U.S. Geological Survey Water-Supply Paper 2254, 263 p.

Hoefs, J., 1980, Stable isotope geochemistry, Second Edition: New York, Springer-Verlag, 208 p.

Lamothe, P.L., Meier, A.M., and Wilson, S.A., 2002, The determination of forty four elements in aqueous samples by inductively coupled plasma–mass spectrometry, Chapter H *in* Taggart, J.E., Jr., ed., Analytical methods for chemical analysis of geologic and other materials: U.S. Geological Survey Open-File Report 02–223, p. H1–H11.

Langmuir, D., and Whittemore, D.O., 1971, Variations in the stability of precipitated ferric oxyhydroxides, *in* Hem, J.D., ed., Nonequilibrium systems in natural water chemistry: American Chemical Society Advances in Chemistry Series 106, p. 208–234.

Lipman, P.W., Steven, T.A., Luedke, R.G., and Burbank, W.S., 1973, Revised volcanic history of the San Juan, Uncompahgre, Silverton, and Lake City calderas in the western San Juan mountains, Colorado: U.S. Geological Survey Journal of Research, v. 1, p. 627–642.

McKnight, D.M., Kimball, B.A., and Bencala, K.E., 1988, Iron photoreduction and oxidation in an acidic mountain stream: Science, v. 240, p. 637–640.

Nordstrom, D.K., and Southam, G., 1997, Geomicrobiology of sulfide oxidation, *in* Banfield, J.F., and Nealson, K.H., eds., Geomicrobiology—Interactions between microbes and minerals: Mineralogical Society of America Reviews in Mineralogy, v. 345, p. 361–390.

Parkhurst, D.L., and Plummer, L.N., 1995, PHREEQEC—A Fortran 77 modeling code for aqueous-mineral solution calculations: U.S. Geological Survey Water-Resources Investigations 23, 45 p.

Plummer, L.N., Prestemon, E.C., and Parkhurst, D.L., 1992, NETPATH—An interactive code for interpreting NET geochemical reactions from chemical and isotopic data along a flow PATH, *in* Kharaka, Y., and Maest, A.S., eds., Proceedings, 7th International Symposium on Water-Rock Interaction, Park City, Utah: Rotterdam, Netherlands, Balkema, p. 239–242.

Schippers, A., and Sand, W., 1999, Bacterial leaching of metal sulfides proceeds by two indirect mechanisms via thiosulfate or via polysulfides and sulfur: Applied and Environmental Microbiology, v. 65, p. 2319–2321.

Singer, P.C., and Stumm, W., 1970, Acidic mine drainage—The rate determining step: Science, v. 167, p. 1121–1123.

Smedley, P.L., and Kinniburgh, D.G., 2002, A review of the source, behaviour, and distribution of arsenic in natural waters: Applied Geochemistry, v. 17, p. 517–568.

Stumm, W., and Morgan, J.J., 1985, Aquatic chemistry—An introduction emphasizing chemical equilibria in natural waters, Third Edition: New York, John Wiley, 834 p.

Theodorakos, P.M., 2002, Colorimetric determination of ferrous iron, Fe(II), in natural water, wastewater, and seawater, Chapter W *in* Taggart, J.E., Jr., ed., Analytical methods for chemical analysis of geologic and other materials: U.S. Geological Survey Open-File Report 02–223, p. W1–W2.

Thomas, H.A., 1942, Bacterial densities from fermentation tube tests: Journal American Water Works Association, v. 34, p. 572.

Till, R., 1974, Statistical methods for the earth scientist: New York, John Wiley, 154 p.

van Veen, W.L., Mulder, E.G., and Deinema, M.H., 1978, The *Sphaerotilus-Leptothrix* Group of bacteria: Microbiological Reviews, v. 42, p. 329–356.

Vaughn, R.B., Stanton, M.R., and Horton, R.J., 1999, A year in the life of a mine dump—A diachronic case study, *in* Proceedings of the 6th International Conference on Tailings and Mine Waste, Ft. Collins, Colo., January 1999: Rotterdam, Netherlands, Balkema, p. 475–484.

Wanty, R.B., 2000, A simple device for measuring differences in hydraulic head between surface water and shallow ground water: U.S. Geological Survey Fact Sheet FS–077–00, 2 p.

Zanker, H., Moll, H., Richter, W., Brendler, V., Hennig, C., Reich, T., Kluge, A., and Huttig, G., 2002, The colloid chemistry of acid rock drainage solution from an abandoned Zn-Pb-Ag mine: Applied Geochemistry, v. 17, p. 633–648.